Current Research in Biotechnology 7 (2024) 100175

Contents lists available at ScienceDirect

Current Research in Biotechnology

journal homepage: www.elsevier.com/locate/crbiot

Unveiling the potential of marine-derived diterpenes from the order Alcyonacea as promising anti-obesity agents

Mohamed A. Tammam [a,*,1], Omnia Aly [b,1], Florbela Pereira [c,1], Aldoushy Mahdy [d], Amr El-Demerdash [e,f,*]

[a] Department of Biochemistry, Faculty of Agriculture, Fayoum University, Fayoum 63514, Egypt
[b] Department of Medical Biochemistry, National Research Centre, Cairo 12622, Egypt
[c] LAQV REQUIMTE, Department of Chemistry, NOVA School of Science and Technology, Universidade Nova de Lisboa, 2829516, Caparica, Portugal
[d] Department of Zoology, Faculty of Science, Al-Azhar University (Assiut Branch), Assiut 71524, Egypt
[e] Division of Organic Chemistry, Department of Chemistry, Faculty of Sciences, Mansoura University, Mansoura 35516, Egypt
[f] Department of Biochemistry and Metabolism, The John Innes Centre, Norwich Research Park, Norwich NR4 7UH, UK

ARTICLE INFO

Keywords:
Anti-obesity
Alcyonacea
Sarcophyton glaucum
Fetuin A
PTP1B
Diterpenes
Virtual screening

ABSTRACT

Metabolic syndrome (MS) represents a global health challenge characterized by various metabolic disorders, including HOMA-IR (insulin resistance), obesity, dyslipidemia, and hypertension. In our pursuit of identifying natural alternatives for the development of effective and safe anti-obesity medications, we examined the potential of the methanolic extract of the Red Sea derived soft coral *Sarcophyton glaucum*, where serum levels of glucose, insulin, HOMA-IR, lipid profile, fetuin A and B, PTP1B (Protein tyrosine phosphatase 1B), adropin and omentin were determined. Furthermore, the expression of the UCP1 (Uncoupling protein 1) and PPARGC1A (Peroxisome proliferator–activated receptor-g coactivator-1a) genes have been assessed, to evaluate the anti-obesity potential of *S. glaucum* organic extract. Our findings demonstrated a significant decrease in glucose, HOMA-IR, cholesterol, triglyceride, LDL-C, fetuin A and B, and PTP1B levels, accompanied by a significant increase in insulin, HDL-C, adropin, omentin, UCP1, and PPARGC1A expression after treatment with the soft coral extract. These promising outcomes can be attributed to the remarkable ingredients present in the extract, which were further supported by histopathological findings. In addition, a virtual screening protocol including molecular docking (MDock) and Structure-Activity Relationships (SARs) of 27 marine diterpenes was also explored to identify potential PTP1B inhibitors targeting simultaneously the catalytic site and allosteric site, as well as fetuin A modulators. Moreover, the six most promising predicted marine diterpenes (**4**, **8**, **9**, **10**, **13** and **14**) were investigated for their pharmacokinetic properties, druglike nature and medicinal chemistry friendliness using the SwissADME platform. Of these, four marine diterpenes (**4**, **8**, **9**, and **10**) were predicted to exhibit the appropriate drug-like properties.

Introduction

Obesity presents a significant and pressing public health challenge on a global scale, contributing to a substantial burden of disability and mortality (The Lancet Public Health, 2023). As highlighted by Chait and den Hartigh, obesity is not simply a condition of excess weight but rather an inflammatory systemic disease linked to diabetes, insulin resistance, cancer, heart disease, and chronic kidney disease, among other metabolic diseases (Chait and den Hartigh, 2020). Adipose tissue (AT), comprising stromal vascular cells and adipocytes, plays a key role in obesity development and metabolic diseases. Sedentary lifestyles and inadequate physical activity are major contributors to the onset of obesity and related conditions. Within AT, various adipokines, secreted by this endocrine organ, are involved in the pathogenesis of multiple illnesses and exert significant impacts on lipid and glucose metabolism (Mohammad et al., 2022).

Fetuin B, a hepatokine protein belonging to the family of cysteine protease inhibitors, is secreted by the liver. It shares about 22 % similarity with the other well-known hepatokine, fetuin A (Rudloff et al., 2021). Wang *et al.* established the involvement of fetuin B in obesity and

* Corresponding authors.
E-mail addresses: mat01@fayoum.edu.eg (M.A. Tammam), a_eldemerdash83@mans.edu.eg, Amr.El-Demerdash@jic.ac.uk (A. El-Demerdash).
[1] These authors are equally contributed,

https://doi.org/10.1016/j.crbiot.2024.100175
Received 3 November 2023; Received in revised form 30 December 2023; Accepted 4 January 2024
Available online 9 January 2024

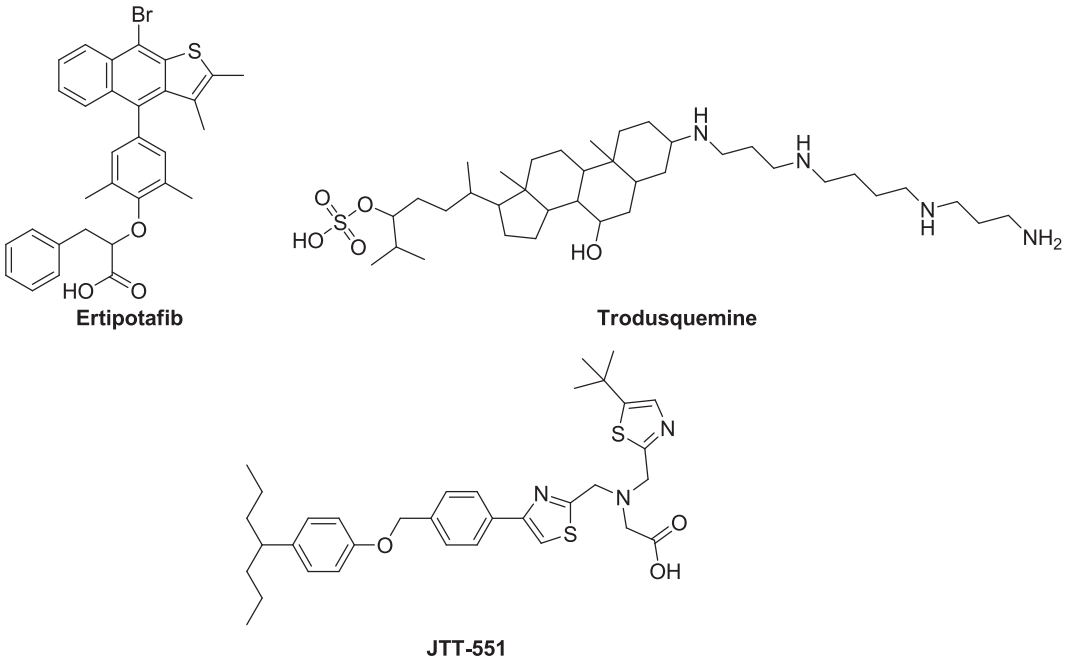

Fig. 1. Chemical structures of small-molecule PTP1B inhibitors investigated in clinical trials (Liu et al., 2022; Sharma et al., 2020).

its related metabolic disorders, i.e., increased levels of fetuin B have been detected in non-alcoholic fatty liver disease, and diabetes, individuals as well as in obese mice. Consistent with these findings, earlier research by the authors revealed a positive correlation between serum fetuin B levels, triglyceride levels, and the risk of insulin resistance in obese Chinese individuals. Furthermore, obese mice treated with recombinant fetuin B exhibited exacerbated liver steatosis and glucose intolerance. In vitro experiments consistently demonstrated that exogenous fetuin B reduces insulin sensitivity in myocytes, hepatocytes, and cardiomyocytes. These results strongly imply that fetuin B is intimately related to insulin resistance and may function as a mediator in obesity-related metabolic disorders. However, the exact pathways through which fetuin B is activated in obesity remain unknown (Wang et al., 2022).

Moreover, adipose tissue and the liver are the primary sources of fetuin A production and secretion. Recent evidence suggests that the liver plays a crucial role in regulating glucose and lipid metabolism through the synthesis of fetuin A, potentially influencing the body's energy homeostasis. In animal models of diet-induced obesity, characterized by hepatic steatosis, an upregulation of fetuin A mRNA expression has been observed in the liver. Multiple cross-sectional and large cohort studies have consistently demonstrated a positive association between elevated fetuin A levels and increased risks of obesity, as well as related conditions such as metabolic syndrome, type 2 diabetes, and both subclinical and clinical cardiovascular disease (CVD). (Ramírez-Vélez et al., 2019).

Protein tyrosine phosphatase 1B (PTP1B) serve as a negative regulator of the phosphorylation and signalling of the insulin receptor (Liu et al., 2022; Sharma et al., 2020; Szczepankiewicz et al., 2003; Wiesmann et al., 2004). Recently, the design of small molecule to treat type II diabetes i.e., PTP1B inhibitors has become increasingly important, due to the fact that the inhibition of PTP1B resulted in the enhancement of insulin action (Liu et al., 2022; Sharma et al., 2020; Yang et al., 2021). Positive charge and high conservation nature of PTP1B catalytic site, motivated the development of PTP1B small molecule inhibitors as a therapeutic drug (Liu et al., 2022; Sharma et al., 2020). Among the conserved residues, Cys 215 and Arg 221 residues are the most vital for the catalysis activity (Liu et al., 2022; Sharma et al., 2020; Szczepankiewicz et al., 2003).

So far, a very limited number of PTP1B inhibitors, including a naphtho[2,3-b]thiophene derivative (ertiprotafib), a synthetic marine amino sterol derivative (trodusquemine) and a bis[(1,3-thiazolyl) methyl]amine derivative (JTT-551), (Fig. 1) have been entered clinical trials, even though the massive efforts undertaken in the investigation of useful PTP1B inhibitors (Liu et al., 2022; Sharma et al., 2020).

Kumar *et al.* identified adropin as a peptide hormone that operates through the G protein-coupled receptor 19 (GPR19) on cell membranes to regulate energy metabolism and insulin resistance (Kumar et al., 2008). Adropin is found in various tissues and organs throughout the body and has been closely associated with obesity and type 2 diabetes (Zhang and Chen, 2022). Additionally, by upregulating the expression of endothelial nitric oxide synthase, it is directly involved in suppressing atherosclerosis. Recent investigations have revealed that this peptide hormone plays a crucial role as a mediator in lipid metabolism, energy balance, and glucose tolerance. It exerts control over lipid and glucose metabolism, thereby offering protection against hyperinsulinemia associated with obesity (Badawy et al., 2020; Ganesh Kumar et al., 2012).

Omentin, an adipocytokine predominantly found in visceral adipose tissue, is known for its anti-inflammatory properties. It has been observed to possess insulin-sensitizing actions, making it a significant factor in regulating lipid metabolism, anti-inflammatory responses, body weight, insulin resistance, and the activation of endothelial nitric oxide synthase. Omentin levels have been found to be lower in people who are insulin resistant and in people who have pro-inflammatory diseases such obesity, type I and type II diabetes (Badawy et al., 2020).

Indeed, through the action of the uncoupling protein 1 (UCP1), brown adipose tissue (BAT) controls energy expenditure by allowing energy to be released as heat. According to several studies, BAT activation is linked to lower blood glucose levels, better insulin resistance, and higher resting energy expenditure in both people and animals. As opposed to subcutaneous adipose tissue (SAT), visceral adipose tissue (VAT) in white adipose tissue (WAT) depots is a more pathogenic depot, and an enlarged VAT is associated with a higher risk of metabolic syndrome and type 2 diabetes mellitus (T2DM) (Bettini et al., 2019).

Strong and versatile transcriptional coactivator, peroxisome proliferator–activated receptor–g coactivator-1a (PPARGC1A gene; PGC-1a protein) controls genes implicated in glucose homeostasis pathways. In

addition to influencing important physiological processes including mitochondrial biogenesis, microvascular flow, and oxidative phosphorylation, PPARGC1A may influence the pathophysiology of type 2 diabetes by affecting important characteristics like insulin function. Data from subcutaneous adipose tissue (SAT) and skeletal muscle support this. Additionally, human subjects exposed to an unfavourable intrauterine environment-that is, individuals with low birth weight and an increased risk of T2D-had increased PPARGC1A methylation in SAT and skeletal muscle, indicating that this gene's epigenetic profile may be susceptible to harmful influences during a person's fatal life (Kelstrup et al., 2016).

Allosteric modulators targeting less conservative allosteric sites are generally more selective and less toxic than orthostatic ligands and thus can achieve better pharmacological profiles (Liu et al., 2022; Sharma et al., 2020; Wiesmann et al., 2004; Yang et al., 2021). An allosteric site of PTP1B was previously recognized by Wiesmann *et al.* and several benzbromarone derivatives have been identified as inhibitors targeting this site; The recognized allosteric site is located away from the catalytic site by 20 Å, and surrounded by α3, α6 and α7 helices in which Leu192, Phe280 and Glu276 residues are the most relevant for allosteric activity (Wiesmann et al., 2004), (Fig. S2 in the Supplementary Material). PTP1B has been implicated in the development of insulin resistance during conditions of metabolic syndrome and obesity (Bourebaba et al., 2021), however, its exact role in controlling adipose tissue biogenesis is still poorly understood. It has also been shown recently that fetuin A, a glycoprotein, is a key regulator of insulin resistance (Bourebaba et al., 2021; Bourebaba and Marycz, 2019), thus representing a promising target for the study and characterization of this process.

Indeed, marine organisms are distinguished with their unusual metabolic and physiological abilities, resulted from their novel and unique secondary metabolites which arose of the distinctive environment they have grown in (Ghareeb et al., 2020; Tammam and El-Demerdash, 2023). In the last decade, marine natural products were found to be a novel supplier of several secondary metabolites that can be an effective substance in several applications either in cosmetology or pharmaceutical (Tammam et al., 2023). Up to now 17 peptides and small molecules already exist in the marine pharmaceutical clinical pipeline, and gained the approvement from US FDA and EMEA, among the approved drugs, vidarabine (Vira-A®; FDA- permitted 1976), trabectedin (Yondelis®; FDA- permitted 2015), and ziconotide (Prialt®, FDA- permitted 2004), for viral, tumor, and pain treatments, respectively.

One unique source of novel and structurally diverse secondary metabolites from the marine environment is the soft corals of the order Alcyonacea, genus *Sarcophyton* (family: Alcyoniidae) (Song et al., 2023; Tammam et al., 2023). Approximately 828 different marine derived natural products were identified from this genus (MarinLit, 2023), mostly including terpenes (Liang and Guo, 2013), steroids (Ngoc et al., 2021), quinones (Huang et al., 2020). Indeed, the genus *Sarcophyton* exhibits remarkable chemical diversity, allowing for the display of a broad range of biological activities. These activities encompass cytotoxicity, anti-inflammatory effects, anti-angiogenic properties, antimicrobial activity, neuroprotective potential, immunomodulatory effects against tumors, antifouling properties, and even ichthyotoxic (Song et al., 2023; Wang et al., 2012).

So far few compounds of natural origin were found to be able to prevent obesity and lower lipids levels through several and different mode of actions, including compounds of plant origin for example curcumin isolated from the rhizomes of *Curcuma longa*, capsaicin which is the major constituent of *Capsicum annuum*, the triterpene derivative celastrol obtained from *Tripterygium wilfordii* roots, the saponin derivative ginsenosides isolated from the rhizomes and roots of *Panax ginseng*, gingerol and shogaol that detected in the extract of ginger (*Zingiber officinale*). Also, marine environment supports us with some compounds with anti-obesity effect for example the sesquiterpene derivative palinurin, callyspongynic acid, dysidine, the anthraquinones derivatives questinol and citreorosein, and the brominated lipid methyl xestospongic ester, phorbaketal A isolated from the marine sponges *Ircinia dendroides*, *Callyspongia truncate*, *Dysidea* sp, *Stylissa flabelliformis*, *Xestospongia testudinaria*, and *Phorbas* sp., respectively; additionally yoshinone A, a C-pyrone derivative obtained from the cyanobacterium *Leptolyngbya* sp and the indole alkaloid derivative meridianin C obtained from the macroalgae *Aplidium meridianum* (Arya et al., 2020).

Furthermore, several diterpenes including abietane-type, pimarane-type, and tenkaurane-type isolated from plants have been reported to be active as PTP1B inhibitors, marine diterpenes that serve as PTP1B inhibitors are rare (Liang et al., 2014). As mentioned in Scheme 1 (Supplementary materials), a couple of diterpenes obtained from different genera of the phylum *Cindaria* displayed either mild or strong effect as PTP1B inhibitors, *e.g.*, sarsolilides A and B, 4*Z*,12*Z*,14*E*-sarcophytolide, ketoemblide, sarcrassin E, cembrene-C, sarcophytonolide N, and methyl sarcotroate B with IC_{50} values ranged from 5.95 to 27 μM (Liang et al., 2014, 2013b, 2013a).

Consequently, we have been motivated to investigate the anti-obesity of the methanolic extract of the Red Sea derived soft coral *S. glaucum* on a HCHFD model for obese rats using biochemical and histological techniques to verify its hypolipidemic effect, supported by a virtual screening protocol including molecular docking (MDock) and Structure-Activity Relationships (SARs) of 27 marine diterpenes to identify potential PTP1B inhibitors targeting simultaneously the allosteric site and catalytic site, as well as fetuin A modulators. For the computational studies, the targets PTP1B and fetuin A were selected, as the first is one of the most attractive targets for therapeutic intervention in the antidiabetic and anti-obesity area and, on the other hand, activity against PTP1B from the library of diterpenes studied was reported. The choice of the second target, fetuin A, was due to the fact that it appears to have a key role in the development of several clinical conditions, such as insulin resistance, type 2 diabetes mellitus, metabolic disorders and non-alcoholic fatty liver disease. The pharmacokinetic properties, druglike nature and medicinal chemistry friendliness were calculated for the six most promising predicted marine diterpenes (**4**, **8**, **9**, **10**, **13** and **14**) using the SwissADME platform. Of these, four marine diterpenes (**4**, **8**, **9** and **10**) were predicted to exhibit the appropriate drug-like properties.

Material and methods

Biological material

The examined marine derived soft coral *S. glaucum*, has been collected in July 2015, from the coast of Hurghada, Egypt, at a depth of 8 m, and transported frozen to the laboratory, and stored at −20 °C, until further analysis.

In vivo examination of the anti-obesity ability of S. glaucum extract

Experimental animals

In this investigation, fifty male albino rats weighing between 180 and 200 g at the start of the trial were taken from the animal house of the author's institution. The rats were kept in separate, hygienic polypropylene cages and kept in a temperature-controlled room (22 ± 2 °C) with a 12-hour light and 12-hour dark cycle. This study used a model that more accurately reflected the alterations seen in human obesity by feeding the animals a Western-style diet, also known as a high-carbohydrate, high-fat (HCHF) diet, as described by (Wilson et al., 2007), is used here to develop a model that better captures the evolution of obesity in humans. The typical diet was cooked in accordance with (Reeves, 1997). Before the trial, the animals were given a period of fourteen days to become used to the laboratory environment. All procedures were approved by the Ethics Committee of the National Research Centre, Dokki, Cairo, Egypt, with approval number (74125062023), and were conducted in accordance with the UK

Animals (Scientific Procedures) Act, 1986 and related guidelines, EU Directive 2010/63/EU for animal experiments, and the National Research Council's Guide for the Care and Use of Laboratory Animals.

Experimental study design (Duration of experiment = 20 weeks)

Five groups (10 rats each) were randomly selected from a pool of fifty male albino rats. Group I (Control group): Normal diets were given to healthy rats. Group II (HCHFD group): A high-carbohydrate, high-fat diet was administered to the rats. Group III (Soft coral group): The soft coral crude extract (20 mg/kg/day) was given orally to healthy rats (Abdel-Wahhab et al., 2012). Group IV (HCHFD + Soft coral group): Rats were given a high-carb, high-fat diet before receiving oral treatment for eight weeks at a dose of 20 mg/kg of soft coral crude extract. Group V (HCHFD + Orlistat group): rats were fed on High carbohydrate High Fat Diet and then treated with orlistat at 10 mg/kg/day, orally (Zaitone and Essawy, 2012) (8 weeks).

Collection of samples

Following the 20-week experimental period, the animals were kept fasting for 8 h prior to blood collection. Blood was extracted using capillary tubes from the retroorbital venous plexus of the eye while the subjects were sedated with formalin, collected in clean tubes, allowed to clot, and centrifuged for 10 min at 3000 r.p.m. The serum was isolated and kept in an Eppendorf container at −20 °C in order to determine its biochemical characteristics. Rats were killed by cervical dislocation after blood samples were taken and stored at −80 °C until they were employed in gene-expression research. The liver and pancreas were preserved in 10 % formalin-phosphate buffered formalin for subsequent pathological evaluation.

Biochemical analysis

The glucose level in serum was determined using standard commercial colorimetric enzymatic tests (BioMerieux, Marcy l'Etoile, France; Roche Diagnostics, Basel, Switzerland) in accordance with the procedures of Passing and Bablok (Passing and Bablok, 1983). Using a kit from BioSoure INSEASIA Co. (Nivelles, Belgium), the enzyme linked immunological sorbent assay described by Yallow and Bawman was used to assess the serum insulin level (Yalow and Bauman W. A, 1983). Insulin resistance was determined using the subsequent formula: According to Mathews et al., the HOMA-IR formula (homeostatic model assessment for insulin resistance) is equal to fasting glucose (mg/dl) × fasting insulin (μIU/ml)/405 (Matthews et al., 1985).

Serum levels of HDL-cholesterol (high density lipoprotein), triglycerides (TG), cholesterol and LDL-cholesterol were measured according to the methods mentioned by Kim *et al.* Cole *et al.* Lopes Virella *et al.* and Friedewald *et al.* respectively (Cole et al., 1984; Friedewald et al., 1972; Kim et al., 2007; Lopes Virella et al., 1977).

The levels of serum fetuin A, fetuin B, and PTP1B were analyzed by means of an ELISA (enzyme-linked immunosorbent assay) using the manufacturers protocols with Catalog Number: LS-F5816-1; E-EL-R2451and EK720896 respectively. Serum omentin and adropin levels, as reported by De Souza Batista *et al.* and Topuz *et al.* were measured using ELISA for rats utilizing the manufacturer's methods (R&D systems) (De Souza Batista et al., 2007; Topuz et al., 2013).

Total RNA was isolated from blood samples with the RNase Kit (Qiagen, Germany) and the primers listed in Table 1.and estimated gene expression levels in accordance with Wilfinger *et al.* (Wilfinger et al., 1997).

Table 1
Primer sequence of β-actin, UCP1 and PPARGC1A genes.

Target	Sequence
β-actin	F: 5′-AGGGAAATCGTGCGTGACAT-3′ R: 5′-GAACCGCTCATTGCCGATAG-3′
UCP1	F: 5′-GTGAAGGTCAGAATGCAAGC-3′ R: 5′-AGGGCCCCCTTCATGAGGTC-3′
PPARGC1A	F: 5′-GCT TGA CTG GCG TCA TTC A-3′ R: 5′-ACA GAG TCT TGG CTG CAC ATG T-3′

The thermal profile consisted of five minutes of initial denaturation at 95 °C, forty-five cycles of denaturation at 95 °C for fifteen seconds, annealing (between 56 and 60 °C) for thirty seconds, and extension at 72 °C for forty-five seconds. Using SyberGreen Master Mix to measure fluorescence, amplified genes were measured. By analyzing melting curves, the specificity of the amplification was kept track of. Fold change in the expression of mRNA was obtained using the method of Livak and Schmittgen, and expression level was determined by QuantStudio 12 K Flex real-time PCR, Applied Biosystems, USA, and evaluated using Taqman PCR assays and reagents, Applied Biosystems (Livak and Schmittgen, 2001).

For all data, mean ± SEM was used. The normal state test (SPSS program, version 26) accustomed to confirming that there was a normal distribution in the data. One way analysis of variance (ANOVA) and post hoc Bonferroni tests (for experiments involving more than two groups and one variable) were used to assess statistical significance. It was possible to find Pearson's correlation coefficient. The significance level (P value) for this experiment was set at less than 0.05 (Levesque, 2005).

Histopathological examination

Liver and pancreas were excised from experimental group and followed by their fixation using a neutral buffered solution of formalin for 48 h. They were subsequently washed in distilled water and processed through graded series of alcohol, cleared in xylene and eventually, embedded in paraffin wax. Sections of 5μ thickness were cut; stained with haematoxylin and eosin and mounted in DPX. Stained sections were examined with light microscope for histopathological disorders. Every field underwent an examination and was categorized based on the degree of alterations: none (−), mild (+), moderate (++), and severe (+++) damage (Paget and Thomson, 1979).

Preparation of the screening library

The optimization of the 3D structure of the 27 marine diterpenes and the two positive controls (one catalytic inhibitor of the protein tyrosine phosphatase 1B (PTP1B), a dinaphthyl derivative (Szczepankiewicz et al., 2003), and one allosteric inhibitor of the PTP1B, a sulphonamide benzbromarone derivative (Wiesmann et al., 2004), was performed with the Gaussian 09 program (Frisch et al., 2010) using the hybrid method B3LYP and the base set 6-31G(d,p) (Becke, 1993a, 1993b). The software program OpenBabel (version 2.3.1) (O'Boyle et al., 2011) was used to convert the SDF files to MOL2 and PDBQT files.

Preparation of the protein structures and molecular docking (MDock)

The 3D X-ray crystal structures of human PTP1B enzyme catalytic site and allosteric site complex with an inhibitor (dinaphthyl and sulphonamide benzbromarone derivatives, respectively) were retrieved from Protein Data Bank, PDB IDs: 1NNY and 1 T49, respectively. A comprehensive homology model of fetuin A (Jumper et al., 2021; Rudloff et al., 2022; Varadi et al., 2022) obtained from the crystal structure of the related protein fetuin B (Cuppari et al., 2019) and generated by AlphaFold2 (https://alphafold.ebi.ac.uk/entry/T1RTK5) was extracted to molecular docking assays. PDBQT files were used for docking to human PTP1B enzyme catalytic site (PDB ID: 1NNY) and allosteric site (PDB ID: 1 T49), as well as fetuin A (AlphaFold Protein Structure Database (PSD) ID: T1RTK5) with AutoDock Vina (version 1.1) (Trott and Olson, 2010). Water molecules, ions and ligands were removed from 1NNY and 1 T49 prior to docking using the AutoDockTools (https://mgltools.scripps.edu/). The coordinates of the search space for PTP1B enzymes (1NNY and 1 T49) were maximized to allow the entire macromolecule to be considered for docking, respectively. The search space coordinates were for 1NYY; Centre X: 27.553 Y: 28.391 Z: 22.074, for 1 T49; Centre X: 56.642 Y: 30.859 Z: 20.526, and

for TIRTK5; Centre X: 1.270 Y: 4.139 Z: 3.694; Dimensions X: 50.000 Y: 50.000 Z: 50.000. Ligand tethering of the PTP1B enzymes and fetuin A protein was performed by regulating the genetic algorithm (GA) parameters, using 10 runs of the GA criteria. The docking binding poses were visualized with PyMOL Molecular Graphics System, Version 2.0 Schrödinger, LLC, UCSF Chimera (Pettersen et al., 2004), and LigPlot^{+} v.2.2.5 (Wallace et al., 1995).

Identification of diterpene library

A library of 27 marine diterpene metabolites (**1**–**27**) were previously described from soft corals, *Sarcophyton solidum*, *Sarcophyton trocheliophorum*, *Sarcophyta elegans*, *Sarcophyton glaucum* and *Sinularia scabra* (Fig. 2, Scheme S1).

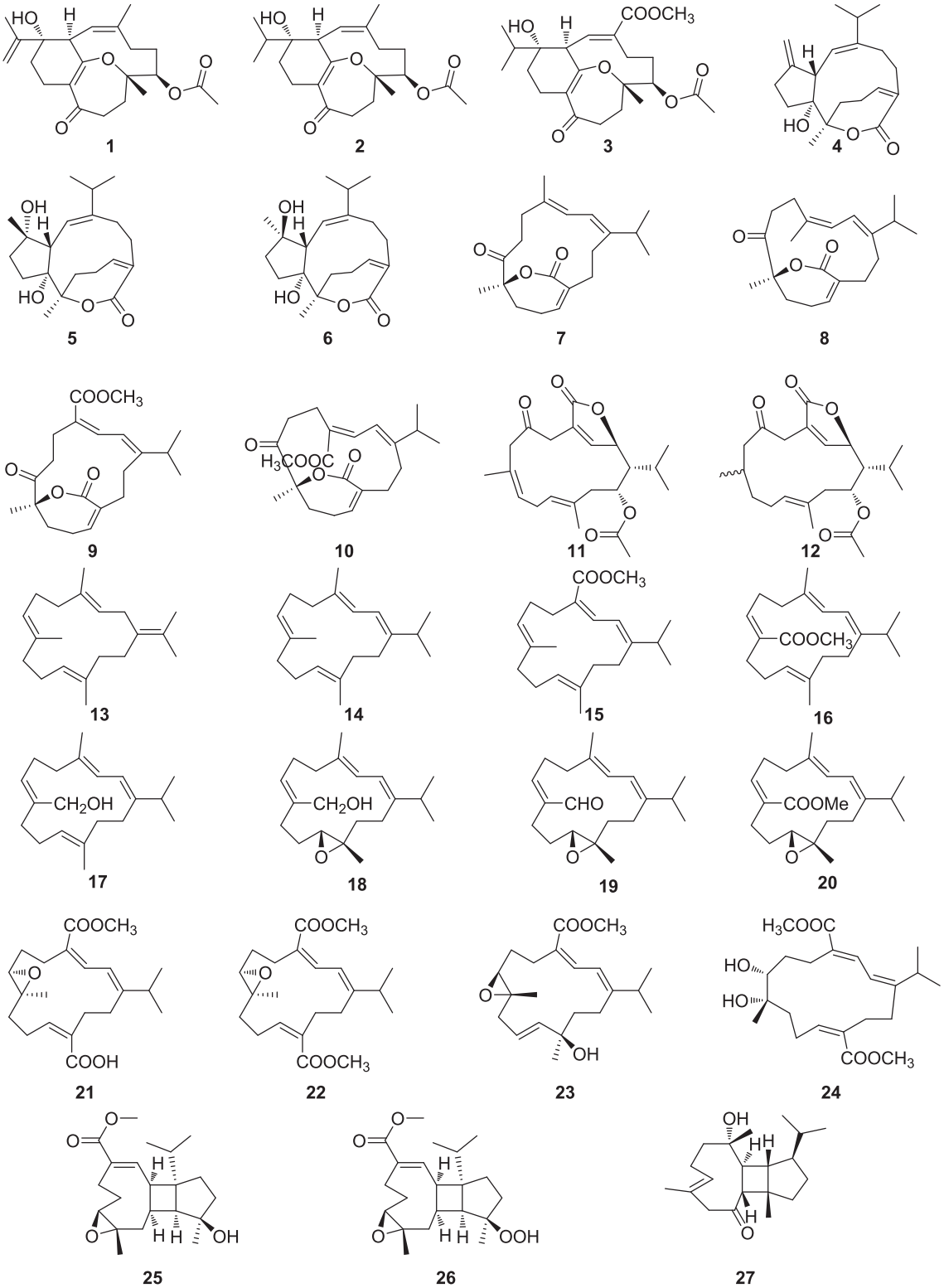

Fig. 2. Examined marine diterpenes **1**–**27**.

Physicochemical properties, pharmacokinetic and toxicity profiles, in-silico prediction

Pharmacokinetic properties, druglike nature and medicinal chemistry friendliness of the six most promising marine diterpenes predicted by MDock and SAR analysis (**4**, **8**, **9**, **10**, **13** and **14**) and the positive controls (dinaphthyl and sulphonamide benzbromarone derivative) were calculated using the SwissADME platform (https://www.swissadme.ch/, accessed on 18 August 2023) (Daina et al., 2017).

Results and discussion

In vivo examination of the anti-obesity ability of S. glaucum extract

The increasing rates of obesity and metabolic syndrome (MS) were mostly brought on by sedentary lifestyles and overeating. Nonetheless, several variables, such as insulin resistance, central obesity, infections, oxidative stress, and genetic predisposition, have contributed to MS's association with obesity. Because multiple sclerosis (MS) affects the entire endocrine system, it can induce anomalies in the body's systems (Gustafsson and Unwin, 2013).

There exist multiple biochemical and genetic variables that may be linked to obesity. Fetuin A and fetuin B are involved in several physiological processes, such as the control of inflammation and insulin resistance (Ramírez-Vélez et al., 2019; Wang et al., 2022). Additionally, PTP1B is an enzyme, has a negative regulatory effect on insulin signalling, it influences how glucose metabolism and insulin resistance are regulated (Liu et al., 2022). Furthermore, while the peptide hormone adropin has been linked to the control of metabolic and energy homeostasis processes (Zhang and Chen, 2022), adipose tissue secretes a protein called omentin, an adipokine, which possesses anti-inflammatory and insulin-sensitizing qualities (Badawy et al., 2020).

Indeed, the results in (Table 2) reflected a significant increase ($P < 0.05$) in fasting blood sugar and HOMA-IR as well as a significant decrease ($P < 0.05$) in insulin level in HCHFD group when compared with control group. While the results showed that fasting blood sugar and HOMA-IR were significant decreased ($P < 0.05$) along with significant elevation ($P < 0.05$) of insulin level in all treated groups compared to the HCHFD group. Additionally, no significant difference was found between the Soft coral group when compared with control group; however, a remarkably large variation was detected between the HCHFD + Soft coral-treated group and Orlistat treated group. Our result reflects that the group received HCHFD + Soft coral showed impressive results in improvement glucose, insulin, and HOMA-IR.

According to our findings which is consistent with previous findings (Badawy et al., 2020), explained that in obese rats, excess adipose tissue contributes to elevated levels of pro-inflammatory cytokines and circulating free fatty acids. These factors can impair glucose uptake and utilization in peripheral tissues, resulting in elevated blood glucose levels and an imbalance between insulin production and insulin sensitivity. Hyperinsulinemia produces more insulin than usual to compensate for decreased insulin sensitivity. However, pancreatic beta cells can become exhausted and insulin production can decrease over time. This is because adipose tissue produces higher levels of inflammatory cytokines, which can interfere with insulin signalling pathways, impairing insulin-stimulated glucose uptake and utilization in target tissues. Multiple variables can contribute to obesity-induced insulin resistance in rats. Chronic low-grade inflammation, altered adipokine secretion from adipose tissue, increased adipose tissue release of free fatty acids, and dysregulated signalling pathways involved in glucose metabolism are all examples (Li et al., 2022).

Additionally, the data in (Table 3) showed that there was a significant increase ($P < 0.05$) in cholesterol, triglyceride, LDL-Cholesterol, and significant decrease ($P < 0.05$) HDL-Cholesterol in HCHFD group when compare with control group. Also, our data showed significant decrease ($P < 0.05$) in cholesterol, triglyceride, LDL-Cholesterol and significant increase ($P < 0.05$) HDL-Cholesterol in all treated groups when compare with HCHFD group. Additionally, no significant difference was found between the Soft coral group and control groups; however, a remarkably large variation was detected. between the HCHFD + Soft coral-treated group and the group treated with orlistat. The groups received Orlistat after induction of obesity showed improved in lipids profile while the group which received the extract of the soft coral after induction of obesity show remarkable progress in lipids profile.

In fact, in obesity, there is an increased release of free fatty acids (FFAs) from adipose tissue due to enhanced lipolysis. These FFAs are taken up by the liver, where they are converted into triglycerides. The increased availability of FFAs and the upregulation of hepatic lipid synthesis contribute to elevated circulating triglyceride levels in obese rats. Additionally, insulin resistance, a common feature of obesity, impairs the ability of insulin to suppress lipolysis in adipose tissue. This further promotes the release of FFAs into the bloodstream, leading to increased triglyceride synthesis in the liver (Jung and Choi, 2014).

Furthermore, very low-density lipoprotein (VLDL) particles are made up of cholesterol, triglycerides, and certain apolipoproteins in the liver. They deliver the fats to the muscle and adipose tissue in the circulation so they can be produced and stored as energy. Triglyceride extraction from low-density lipoprotein (VLDL) eventually transforms the particle into low-density lipoprotein (LDL), which is primarily ApoB-100 and high in free and esterified cholesterol. In addition to carrying cholesterol

Table 2
Fasting glucose, insulin, and HOMA-IR in the examined groups.

	Control	HCHFD	Soft coral	HCHFD + Soft coral	HCHFD + Orlistat
Glucose (mg/dl)	84.79 ± 0.9	178.87 ± 2.81 ^{a}	89.42 ± 0.89^{b}	111.98 ± 2.8 ^{ab}	139.55 ± 1.16 ^{abc}
Insulin (μIU/ml)	14.47 ± 0.23	11.47 ± 0.08 ^{a}	13.76 ± 0.36^{b}	12.97 ± 0.15 ^{ab}	11.02 ± 0.15 ^{abc}
HOMA-IR	3.03 ± 0.06	5.06 ± 0.07 ^{a}	3.04 ± 0.10^{b}	3.59 ± 0.11 ^{ab}	3.79 ± 0.07 ^{ab}

Values are expressed as mean ± standard error (SE), $n = 10$ rats, in each group, a, b, and c significant at $P < 0.05$, when compared with control, HCHFD, and HCHFD + Soft coral, HCHFD, respectively.

Table 3
Lipids profile of the examined groups.

	Control	HCHFD	Soft coral	HCHFD + Soft coral	HCHFD + Orlistat
Cholesterol (mg/dl)	90.72 ± 1.53	164.3 ± 2.2 ^{a}	88.93 ± 1.2^{b}	113.45 ± 1.73 ^{ab}	140.07 ± 1.2 ^{abc}
Triglyceride (mg/dl)	70.53 ± 0.38	167.07 ± 1.52 ^{a}	73.39 ± 0.95^{b}	92.87 ± 0.54 ^{ab}	112.64 ± 0.65 ^{abc}
HDL (mg/dl)	57.31 ± 0.37	24.27 ± 0.33 ^{a}	59.45 ± 0.23 ^{ab}	47.97 ± 0.30 ^{ab}	41.23 ± 0.30 ^{abc}
LDL (mg/dl)	61.95 ± 0.80	116.62 ± 2.15 ^{a}	66.61 ± 0.37^{b}	76.31 ± 1.48 ^{ab}	96.91 ± 1.69 ^{abc}

Values are expressed as mean ± SE, $n = 10$ rats, in each group, a, b, and c, significant at $P < 0.05$, when compared with control, HCHFD, and HCHFD + Soft coral, respectively.

to the periphery, LDL also collects in the arterial wall beneath defective endothelium, together with VLDL and chylomicron remnant particles. A crucial initial stage in the development of atherosclerotic lesions is endothelial dysfunction, which results in a weakened endothelium barrier and produces pro-inflammatory cytokines, chemokines, and reactive oxygen species (ROS) in addition to pro-inflammatory leukocyte adhesion, recruitment, and subendothelial transmigration (Soppert et al., 2020).

Also, HDL cholesterol often referred to as "good cholesterol," plays a protective role in cardiovascular health through cholesterol transportation from peripheral tissues back to the liver for excretion. In obese rats, HDL cholesterol levels are often decreased due to altered lipoprotein metabolism, reduced adipokine secretion and increase inflammation and oxidative stress (Weber and Noels, 2011).

Eventually, these mechanisms collectively contribute to the altered lipid profile observed in obese rats, characterized by increased circulating levels of triglycerides, total cholesterol, and LDL-C, as well as decreased HDL-Cholesterol levels in HCHFD group when compared with control group as showed in Table 3. These lipid profile changes are associated with an increased risk of cardiovascular diseases, including atherosclerosis and coronary artery disease. Lipid profile showed significant improvement after treatment but the result of soft coral outperformed orlistat by far.

In addition, there was a statistically significant rise ($P < 0.05$), as seen in (Table 4) in fetuin A, fetuin B, PTP1B and significant decrease ($P < 0.05$) of adropin and omentin in HCHFD group when compare with control group. Also, our data showed significant decrease ($P < 0.05$) in fetuin A, fetuin B, PTP1B and significant increase ($P < 0.05$) adropin and omentin in all treated groups when compare with HCHFD group. Additionally, no significant difference was found between the Soft coral group and control groups; however, very discernible differences were found between the HCHFD + Soft coral-treated group and orlistat treated group. The groups received Orlistat after induction of obesity showed improved in this marker while the group which received Soft coral after induction of obesity show remarkable progress.

Actually, fetuin A and fetuin B are two similar proteins examined in the context of obesity and metabolic disorders. While fetuin A has received more attention, research on the exact mechanisms of fetuin B in obese mice remains restricted. In obesity, fetuin A has been linked to insulin resistance and metabolic dysfunction development. Impairment of insulin signalling: fetuin A could disrupt the receptor signalling of insulin in peripheral tissues like adipose tissue and skeletal muscle. This reduces insulin sensitivity and contributes to insulin resistance, which is a defining feature of obesity. It has also been linked to persistent low-grade inflammation and has been proven to stimulate this inflammatory response. It can cause adipose tissue and other cells to generate pro-inflammatory cytokines. This inflammation aggravates insulin resistance and metabolic dysfunction even more (Poloczek et al., 2021). Indeed, fetuin A has been shown to inhibit triglyceride breakdown and promote fatty acid synthesis in the liver, resulting in hepatic triglyceride accumulation and the development of non-alcoholic fatty liver disease (NAFLD). It can also contribute to adipose tissue dysfunction, including impaired adipogenesis and adipocyte inflammation (Stygar et al., 2018).

Additionally, fetuin B is a protein that is linked to fetuin A, but its exact role and processes in obesity remain unknown. According to preliminary study, fetuin B may play a role in lipid metabolism and homeostasis. It is thought to affect fatty acid intake and storage in adipose tissue as well as hepatic lipid metabolism. It has also been proposed that fetuin B is involved in energy regulation balance and body weight. Although the specific mechanisms are not well understood, it has been postulated that fetuin B may influence food intake, energy expenditure, or both (Poloczek et al., 2021).

In fact, obesity is often associated with insulin resistance, a condition in which cells become less responsive to insulin, leading to impaired glucose metabolism. PTP1B is known to negatively regulate insulin signalling by dephosphorylating key components of the insulin receptor signalling pathway. By dephosphorylating these components, PTP1B reduces insulin sensitivity and contributes to insulin resistance. Several studies have reported increased PTP1B expression and activity in various tissues of obese rats, including adipose tissue, liver, and skeletal muscle. The upregulation of PTP1B in these tissues is believed to contribute to the development and maintenance of insulin resistance in obesity (Sohail et al., 2022).

Furthermore, adropin protected against obesity-associated hyperinsulinemia and hepatosteatosis by regulating the lipid and glucose metabolism. The mechanism underlying adropin's favourable effects on endothelial function has been proposed: serum adropin boosted nitric oxide generation and bioavailability, hence improving arterial stiffness (Badawy et al., 2020), this study revealed that adropin level was decreased in HCHF group significantly compared to the control. After, treatment its level was significantly increased but the group received soft coral extract showed results more butter than orlistat (Table 4).

Additionally, omentin plays a major role in many pathophysiological processes, including the control of vascular endothelial function, obesity, insulin resistance, inflammatory response, and atherogenesis (Badawy et al., 2020). Omentin levels have been found to be lower in insulin-resistant and pro-inflammatory situations (obesity and types I and II of diabetes mellitus), according to Zengi et al., (Zengi et al., 2019). When comparing the HCHFD group to the control group, the data in (Table 4) demonstrated a substantial drop in omentin. Moreover, there was a noteworthy rise in every treated group as compared to the HCHFD group.

Furthermore, omentin has been demonstrated to increase insulin sensitivity in skeletal muscle, liver, and adipose tissue. It improves insulin signalling by activating the pathway of insulin receptor substrate-1 (IRS-1)/PI3K/Akt. This increases glucose absorption and utilization in peripheral tissues, improving glucose homeostasis and decreasing insulin resistance. It also has anti-inflammatory qualities by inhibiting the generation of pro-inflammatory cytokines and helps to regulate lipid metabolism in obese rats. Omentin has been shown to affect lipid absorption, storage, and utilization in adipose and peripheral tissues. Also, omentin may increase lipolysis, or the breakdown of stored triglycerides, while inhibiting adipogenesis, or the development of new fat cells (Tan et al., 2008).

Additionally, omentin has been linked to the regulation of endothelial function, which is critical for vascular health. It increases nitric

Table 4
Serum levels of fetuin A, fetuin B, PTP1B, adropin and omentin in different examined groups.

	Control	HCHFD	Soft coral	HCHFD + Soft coral	HCHFD + Orlistat
Fetuin A	33.01 ± 0.72	75.70 ± 0.82 [a]	30.83 ± 0.31[b]	44.87 ± 0.26 [ab]	53.32 ± 0.53 [abc]
Fetuin B	80.40 ± 1.10	138.84 ± 1.71 [a]	74.17 ± 0.92 [ab]	90.00 ± 1.01 [ab]	118.62 ± 1.17 [abc]
PTP1B (ng/mL)	0.53 ± 0.02	3.59 ± 0.09 [a]	0.50 ± 0.02[b]	1.76 ± 0.02 [ab]	2.83 ± 0.07 [abc]
Adropin (ng/ml)	854.80 ± 6.76	623.40 ± 1.85 [a]	900.30 ± 2.00[b]	722.70 ± 4.63[b]	655.5 ± 4.07 [ac]
Omentin (pg/ml)	17.54 ± 0.19	5.38 ± 0.12 [a]	18.65 ± 0.16[b]	14.22 ± 0.47 [ab]	10.46 ± 0.24 [abc]

Values are expressed as mean ± SE, $n = 10$ rats, in each group, a, b, and c, significant at $P < 0.05$, when compared with control, HCHFD, and HCHFD + Soft coral, respectively.

Table 5
mRNA fold change for the expression of UCP1 and PPARGC1A genes by RT-qPCR in different examined groups.

	Control	HCHFD	Soft coral	HCHFD + Soft coral	HCHFD + Orlistat
UCP1	1.00 ± 0.00	0.40 ± 0.01 [a]	1.29 ± 0.08 [ab]	6.37 ± 0.09 [ab]	5.27 ± 0.06 [abc]
PPARGC1A	1.00 ± 0.00	0.33 ± 0.01 [a]	1.52 ± 0.07 [ab]	5.69 ± 0.05 [ab]	4.55 ± 0.06 [abc]

Values are expressed as mean ± SE, $n = 10$ rats, in each group, a, b, and c, significant at $P < 0.05$, when compared with control, HCHFD, and HCHFD + Soft coral, respectively.

oxide (NO) generation, a vasodilator that enhances blood flow and endothelial function. Omentin may help attenuate the cardiovascular problems associated with obesity by increasing NO production and decreasing endothelial dysfunction. While, it has been proposed that it influences energy expenditure and thermogenesis, or the creation of heat by adipose tissue. It may improve mitochondrial activity and boost the expression of energy-related genes such as uncoupling protein 1 (UCP1). These changes could potentially help regulate body weight and metabolic rate in obese rats (Hayashi et al., 2019). In addition, as shown in (Table 5), there was a statistically significant drop ($P > 0.05$) in UCP1 and PPARGC1A genes fold change expression in HCHFD group when compare with control group. The group which received orlistat after induction of obesity showed improvement in results while the group received soft coral showed promising result.

Indeed, Reduced expression of the UCP1 (Uncoupling Protein 1) gene, which is largely expressed in brown adipose tissue (BAT), may have several dangers or adverse effects. Therefore, UCP1 is essential for thermogenesis and energy expenditure, and altering its expression can affect metabolic control (Schirinzi et al., 2023). As illustrated, in Table 5, a significant decrease in UCP1 expression in the HCHFD group compared to the control group can impede thermogenesis in brown adipose tissue, potentially lowering the ability to generate heat in response to cold exposure or diet-induced thermogenesis, UCP1 oversees decoupling mitochondrial respiration from ATP production, which results in heat generation rather than energy storage. Furthermore, because UCP1-mediated thermogenesis contributes to overall energy expenditure, decreasing UCP1 expression may result in decreased energy expenditure, potentially leading to a reduced metabolic rate and an increased susceptibility to weight gain or obesity. Also Reduced UCP1 expression may have an impact on lipid utilization and storage in BAT, potentially resulting in dysregulation of lipid metabolism and abnormalities in circulating lipid profiles. Activation of UCP1 has been linked to improved glucose homeostasis, including greater glucose absorption and insulin sensitivity. Reduced UCP1 expression may impair glucose metabolism, potentially leading to decreased glucose tolerance and insulin resistance. Moreover, lower UCP1 levels may result in less energy dissipation, more energy storage, and a tendency for weight gain and obesity. Eventually, reduced UCP1 expression may trigger compensatory mechanisms in other tissues or metabolic pathways, altering the overall metabolic balance and causing unforeseen effects (Maliszewska and Kretowski, 2021).

Additionally, as compared to the control group, our results demonstrated a substantial decrease in PPARGC1A in the HCHFD group, and following treatment, its level improved (Table 5). PPARGC1A regulates various critical processes in human bodies, including energy metabolism and adaptive thermogenesis, as well as mitochondrial biogenesis and function. A lack of PPARGC1A may impair mitochondrial function, leading to decreased energy metabolism and increased oxidative stress. It regulates the expression of genes involved in gluconeogenesis, fatty acid oxidation, and lipogenesis, in addition to its role in glucose and lipid metabolism; and so, reducing its levels may interfere with glucose and lipid metabolism, resulting in insulin resistance and dyslipidaemia. Furthermore, because it is involved in the control of adaptive thermogenesis, such as the browning of white adipose tissue (WAT) and activation of brown adipose tissue (BAT), lowering its level may limit thermogenesis, resulting in decreased energy expenditure and increased obesity. It has also been shown to have anti-inflammatory capabilities, and a lack of it is linked to increased inflammation in a range of metabolic tissues. so PPARGC1A expression or activity levels that are low may contribute to the development and progression of metabolic disorders. Finally, because PPARGC1A interacts with a variety of transcription factors and signalling pathways involved in energy metabolism and cellular homeostasis, it is possible that it has off-target effects (Huang et al., 2023).

The histological results (Table 6 and Fig. 3) corroborated our biochemical findings. The control group's pancreatic sections displayed normal islets of Langerhans (Islets) with pale, rounded, and ovoid cells in the centre, embedded in the pancreatic exocrine region (Fig. 3A). Examining the pancreas section from the HCHFD group revealed that the endocrine and exocrine glands were disorganised, and the islets of Langerhans (Islet) had shrunk. It was also evident that the exocrine acini's vacuolation, degeneration, and fatty changes had caused a slight dilatation of the ductal tissue, and that there had been mild inflammatory cell infiltration. (Fig. 3B). Furthermore, analysis of pancreatic sections of the group treated with the soft coral, revealed an almost typical islet organisation with centrally located cells and exocrine acini (Fig. 3C). The islets of Langerhans in the pancreatic sections of the soft coral group and HCHFD were determined to be almost normal. While some pancreatic acini are almost normal, others (arrowhead) are still degenerating. There is an invasion of moderately inflammatory cells within certain blocked blood vessels (Fig. 3D). Improvements in pancreatic tissue structure were observed in the inspection section for the HCHFD and Orlistat groups. This was demonstrated by the restoration of normal pancreatic architecture, pancreatic islets size (Islet), with

Table 6
Semi-quantitative recording of architectural disfunction on histopathological examination of the pancreas of different examined groups.

	Control	HCHFD	Soft coral	HCHFD + Soft coral	HCHFD + Orlistat
Shrinkage of islets of Langerhans	–	++	–	–	+
Degeneration and necrosis	–	++	–	+	+
Vacuolation	–	++	–	–	–
Pyknotic nuclei	–	++	–	+	+
Fatty changes	–	+++	+	–	–

Histological grading was made according to four severity grades: – (none); + (mild); ++ (moderate) and +++ (severe).

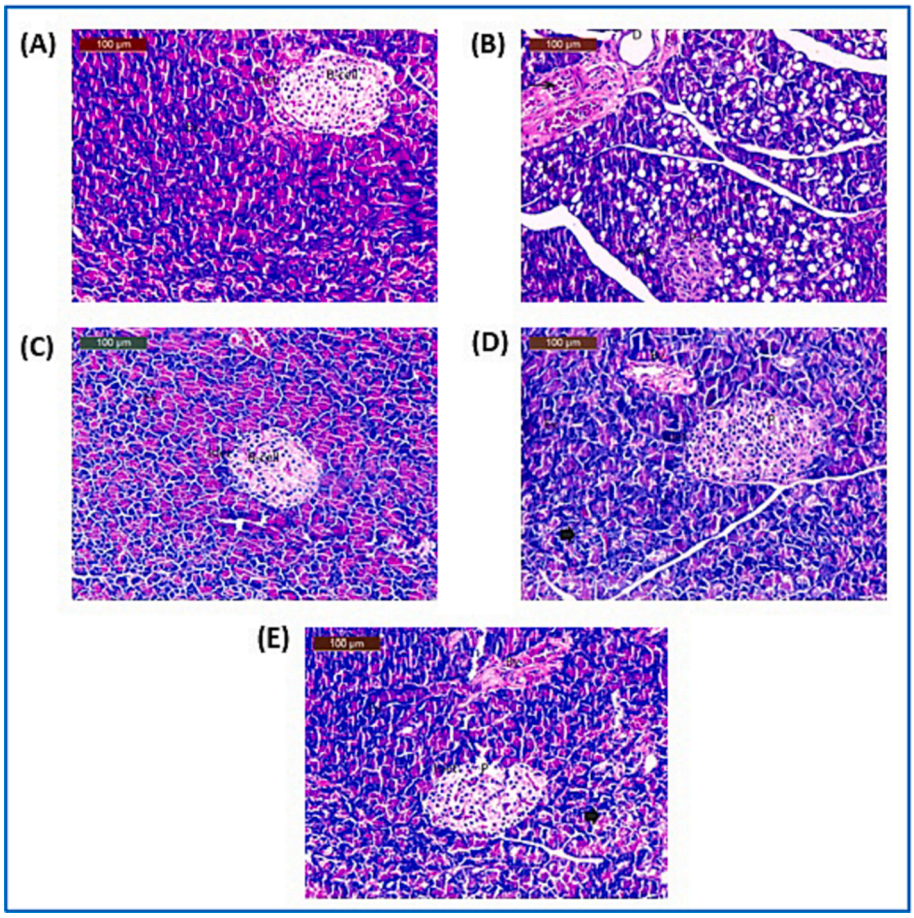

Fig. 3. A photomicrograph of rat pancreas (A) control group, (B) HCHFD group, (C) soft coral group, (D) HCHFD + soft coral group and (E) HCHFD + Orlistat group.

Table 7
Semi-quantitative recording of architectural disfunction on histopathological examination of the liver of different examined groups.

	Control	HCHFD	Soft coral	HCHFD + Soft coral	HCHFD + Orlistat
Hepatic necrosis	–	++	–	+	+
Inflammatory infiltration	–	++	–	–	–
Congestion and dilatation of sinusoids	–	++	–	–	+
Pyknotic nuclei	–	++	–	+	+
Fatty changes	–	+++	+	+	–

Four severity scores were used for histological grading: – (none); + (mild); ++ (moderate); and +++ (severe).

few pyknotic nuclei and virtually normal exocrine acini, while other still degenerated. A few blood vessels are obstructed (Fig. 3E).

Table 7 and, Fig. 4, showed the results of the histopathological examination of livers of the different examined groups. The liver slices from the control group had hepatocytes organised in cords that extended from the central veins, with spherical vesicles containing blood sinusoids in their nuclei (Fig. 4A). The hepatic tissues of the HCHFD group were subjected to histological examination, which revealed necrosis, fatty cells, degenerative alterations close to the central vein, mononuclear cell infiltration, focal mononuclear cell infiltration with pyknotic nuclei, and modest Kupffer cell activation (Fig. 4B). Conversely, soft coral group, showed nearly normal morphology along with very low activation of Kupffer cells (Fig. 4C). Liver tissue sections from the HCHFD and soft coral groups showed essentially normal structure with a few fatty cells with pyknotic nuclei, slightly dilated blood sinusoids, and mildly worsening changes around the major vein (Fig. 4D). Furthermore, a portion of liver tissue from the HCHFD and Orlistat groups showed primarily normal structure with a few fatty cells with pyknotic nuclei, moderately stimulated Kupffer cells, and slightly dilated blood sinusoids (Fig. 4E).

Molecular docking (MDock), binding energies studies and Structure-Activity Relationships (SARs) analysis

Molecular docking was applied to elucidate the binding action of 27 marine diterpene derivatives against human PTP1B enzyme catalytic (PDB ID: 1NNY) and allosteric (PDB ID: 1 T49) sites and fetuin A (AlphaFold PSD ID: T1RTK5) for the treatment of type2 diabetes and obesity. The marine diterpene dataset comprises: 2 tetracyclic

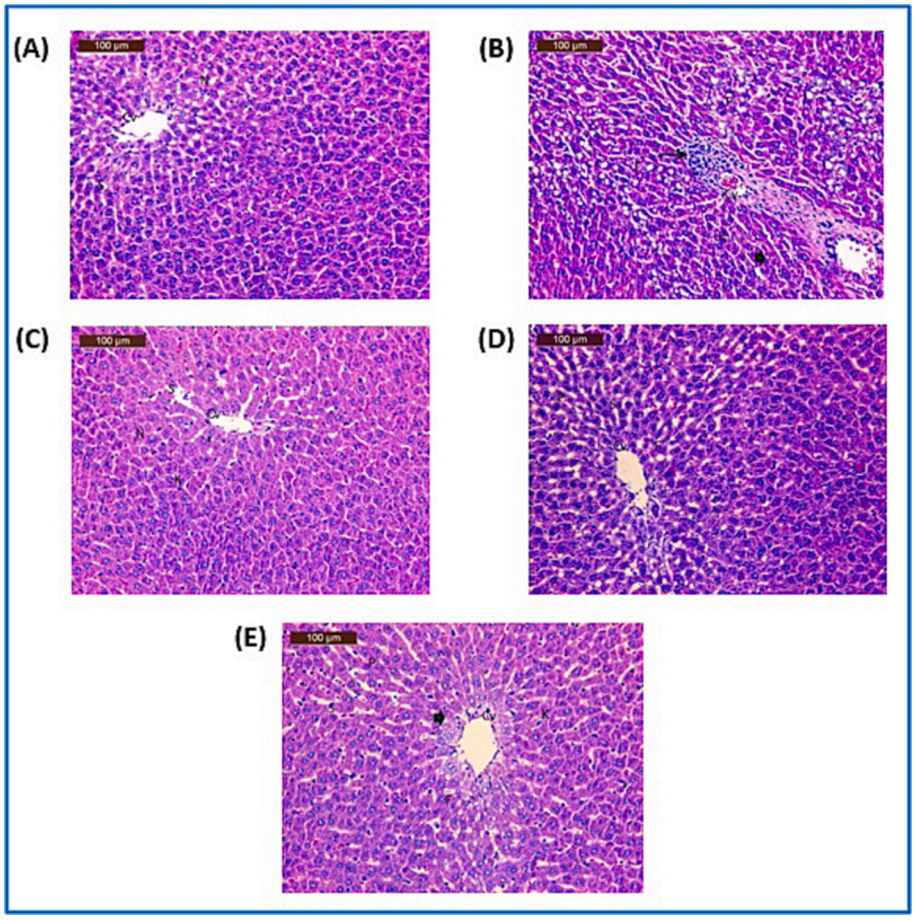

Fig. 4. A photomicrograph of rat liver (A) control group, (B) HCHFD group, (C) soft coral group, (D) HCHFD + soft coral group and (E) HCHFD + Orlistat group.

diterpenes with core **IX** (**25** and **26**), 7 tricyclic diterpenes with cores **I-II-X** (**1**–**6** and **27**), 12 bicyclic diterpenes with cores **III-IV-VI-VII** (**7**–**12** and **18**–**23**), and 6 monocyclic diterpenes with cores **V-VIII** (**13**–**17** and **24**), Scheme 1. In Table 8, the results of molecular docking using the AutoDock Vina software on PTP1B enzyme (catalytic and allosteric sites) and fetuin A were represented.

As shown in Fig. 5 the best-docked poses for the positive controls, dinaphthyl and sulphonamide benzbromarone derivatives, were shown on PTP1B enzyme catalytic and allosteric sites.

Fig. 5, shows the catalytic and allosteric sites of PTP1B, which are defined by residues Cys215 and Leu192-Phe280-Glu276, respectively (Liu et al., 2022; Sharma et al., 2020; Yang et al., 2021). Besides this catalytic site (named as A), there are three additional secondary aryl phosphorylation binding sites that were identified and named as B, C, and D sites (Liu et al., 2022). The B site is a specific lipophilic and involves mainly residues Tyr20, Arg24, Ala27, Phe52 Arg254 and Met258 - Gly259 (Liu et al., 2022). The C and D sites are charged region and are mainly formed by residues Tyr46-Arg47-Asp48 and Tyr46-Glu115-Lys120-Asp181-Ser216, respectively (Liu et al., 2022). According to the extended four-site-based binding mode (Fig. 5A), the PTP1B inhibitors (dinaphthyl and sulphonamide benzbromarone derivatives) can be divided into two different types, ADC (binding to A, D, and C sites) and AD (binding to A and D sites), respectively. Fig. 5A (left side) and Fig. S3 (Supplementary Material) show a clear interaction between the residue of A site (Cys215), the residues of D site (Tyr46-Lys120-Ser216) and the residues of C site (Tyr46-Asp48) of PTP1B with dinaphthyl derivative. The hydrophobic interactions of the terminal naphthyl ring in dinaphthyl derivative with residues Cys215 and Ser216 of the PTP1B enzyme appear to be very relevant, Fig. 5A and Fig. S3. The other naphthyl moiety and the acetamide substitute of the dinaphthyl derivative appear to participate in hydrophobic interactions with residue Tyr46 and Asp48, respectively (Fig. 5A, left side). On the other hand, the oxygen atoms on the *N*-phenylbenzene sulphonamide group of the sulphonamide benzbromarone derivative appears to participate in hydrophobic interactions with residues Cys215, Lys120 and Ser216, see Fig. 5A (right side) and Fig. S4 (Supplementary Material). The hydrophobic interactions of the ethyl substituent on benzofuran ring in sulphonamide benzbromarone derivative with residue Asp181 of the PTP1B enzyme appear to be also relevant, Fig. 5A and Fig S4.

Fig. 5B shows a clear interaction between the residues Leu192-Phe280-Glu276 of the allosteric site with dinaphthyl (left side) and sulphonamide benzbromarone (right side) derivatives. The hydrophobic interactions of the terminal naphthyl ring, the methyl group on the acetamide group and the phenyl ring in dinaphthyl derivative with residues Leu192, Phe280 and Glu276 of the PTP1B enzyme, respectively, appear to be very relevant, Fig. 5B and Fig. S5. Likewise, the

Table 8
Calculated free binding energies (ΔG_B, in kcal/mol) of the investigated 27 marine diterpenes and the positive controls (a dinaphthyl and a sulphonamide benzbromarone derivatives) against PTP1B (catalytic and allosteric sites) and fetuin A.

Marine diterpenes	PTP1B $\Delta G_B^{b,c}$, in kcal/mol		Fetuin A $\Delta G_B^{b,c}$, in kcal/mol
	Catalytic site	Allosteric site	
1	−6.90 ± 0.00	−5.66 ± 0.05	−5.93 ± 0.24
2	−7.06 ± 0.05	−5.88 ± 0.07	−5.85 ± 0.25
3	−6.70 ± 0.09	−5.50 ± 0.09	−5.40 ± 0.10
4	**−7.50 ± 0.00**[d]	**−7.40 ± 0.00** [d]	−5.75 ± 0.05
5	−7.08 ± 0.04	−6.20 ± 0.00	−5.70 ± 0.00
6	−7.10 ± 0.00	−6.10 ± 0.00	−5.60 ± 0.00
7	−7.10 ± 0.00	−6.70 ± 0.00	−5.55 ± 0.15
8	**−7.40 ± 0.00** [d]	**−7.00 ± 0.00** [d]	−5.70 ± 0.00
9	**−7.30 ± 0.00** [d]	−6.88 ± 0.04	−5.70 ± 0.10
10	**−7.28 ± 0.04** [d]	−6.88 ± 0.04	−5.75 ± 0.05
11	−7.00 ± 0.00	−6.50 ± 0.13	−6.05 ± 0.05
12	−6.60 ± 0.00	−5.94 ± 0.12	−6.00 ± 0.20
13	**−7.20 ± 0.00** [d]	−6.40 ± 0.00	−5.55 ± 0.05
14	**−7.24 ± 0.05** [d]	−6.46 ± 0.28	−5.10 ± 0.00
15	−6.40 ± 0.00	−6.12 ± 0.04	−5.65 ± 0.05
16	−6.56 ± 0.05	−6.34 ± 0.05	−5.50 ± 0.10
17	−6.88 ± 0.12	−6.00 ± 0.00	−5.30 ± 0.00
18	−6.32 ± 0.04	−5.84 ± 0.05	−5.30 ± 0.00
19	−6.30 ± 0.00	−5.96 ± 0.05	−5.30 ± 0.00
20	−6.80 ± 0.11	−5.96 ± 0.05	−5.45 ± 0.05
21	−6.34 ± 0.05	−5.80 ± 0.13	−5.50 ± 0.00
22	−6.08 ± 0.04	−5.90 ± 0.00	−5.40 ± 0.20
23	−6.62 ± 0.10	−5.50 ± 0.00	−5.30 ± 0.00
24	−6.06 ± 0.05	−5.70 ± 0.00	−5.40 ± 0.20
25	−6.90 ± 0.00	−6.52 ± 0.04	−5.50 ± 0.00
26	−7.10 ± 0.09	−6.30 ± 0.00	−5.80 ± 0.00
27	−6.70 ± 0.00	−6.38 ± 0.04	−5.25 ± 0.05
Dinaphthyl derivative[a]	−7.10 ± 0.09	−8.20 ± 0.28	−5.45 ± 0.15
Sulphonamide benzbromarone derivative[a]	−7.58 ± 0.11	−8.66 ± 0.05	−6.80 ± 0.30

[a] Positive control. [b] Average of five molecular docking replicates. [c] Standard deviation value verified between the molecular docking replicates for each ligand docked. [d] The diterpenes selected (**highlighted in bold blue**) have a calculated ΔG_B < -7.10 kcal/mol and −6.90 kcal/mol for PTP1B enzyme catalytic and allosteric sites, respectively.

oxygen atom of the ketone group, the oxygen atom in the benzofuran ring, and the phenyl ring in the benzene sulphonamide moiety of the sulphonamide derivative benzbromarone appear to participate in hydrophobic interactions with residues Leu192, Phe280, and Glu276, respectively, see Fig. 5B (right side) and Fig. S6 (Supplementary Material).

As shown in Table 7 and Scheme 1, all the marine diterpene derivatives selected to be the most promising PTP1B inhibitors are from cores II (**4**), III (**8**,**9** and **10**) and V (**13** and **14**). Of these, only two derivatives are simultaneously the most promise catalytic and allosteric site inhibitors, derivatives (**4**) and (**8**). The two diterpenes, (**4**) and (**8**), from cores II and III, respectively, present an α,β-unsaturated ε-caprolactone fused to a cyclic system, Scheme S1.

The marine diterpenes with the lowest ΔG_B calculated for the catalytic and allosteric site, i.e., the most promising derivatives, are 4 and 8 with values of −7.5 and −7.4 kcal/mol for the catalytic site and −7.4 and −7.0 kcal/mol for the allosteric site, respectively (Table 8). Also, it worth mentions that the positive control (dinaphthyl and sulphonamide benzbromarone derivatives), known as catalytic and allosteric inhibitors, respectively, have a ΔG_B values calculated of −7.1 and −7.6 kcal/mol for the catalytic site and −8.2 and −8.7 for the allosteric site, respectively (Table 8). On the contrary, the diterpene derivatives with the highest ΔG_B calculated for the allosteric site, i.e., the least promising derivatives, were (**1**–**3**), and (**18**–**24**) with values between −5.5 kcal/mol and −5.96 kcal/mol (Table 8). Interestingly, all the diterpene derivatives proposed as more promising have an α,β-unsaturated ε-caprolactone ring and, on the other hand, none of the diterpene derivatives predicted to be less active have this moiety. But on the other hand, almost all derivatives predicted to be less promising have a cyclic ether in their structure, *e.g.,* derivatives (**1**–**3**) have a fused tetrahydrooxepinone ring and derivatives (**18**–**23**) have an epoxide ring.

As shown in Fig. 6, the interaction profiles of the best-docked poses for the marine diterpene (**4**) and (**8**) with catalytic and allosteric site of PTP1B enzyme were represented.

According to the catalytic binding mode based on four extended sites (A-D), the two selected diterpene derivatives (**4** and **8**) can be classified as being of the ADC type (binding to sites A, D and C). Fig. 6A (left and right sides) show a clear interaction between the residue of A site (Arg221), the residues of D site (Tyr46-Lys120-Ser216) and the residues of C site (Tyr46) of PTP1B with diterpenes (**4**) and (**8**). As verified with the positive controls, dinaphthyl and sulphonamide benzbromarone derivatives (Fig. 5B), in the case of the two diterpene derivatives

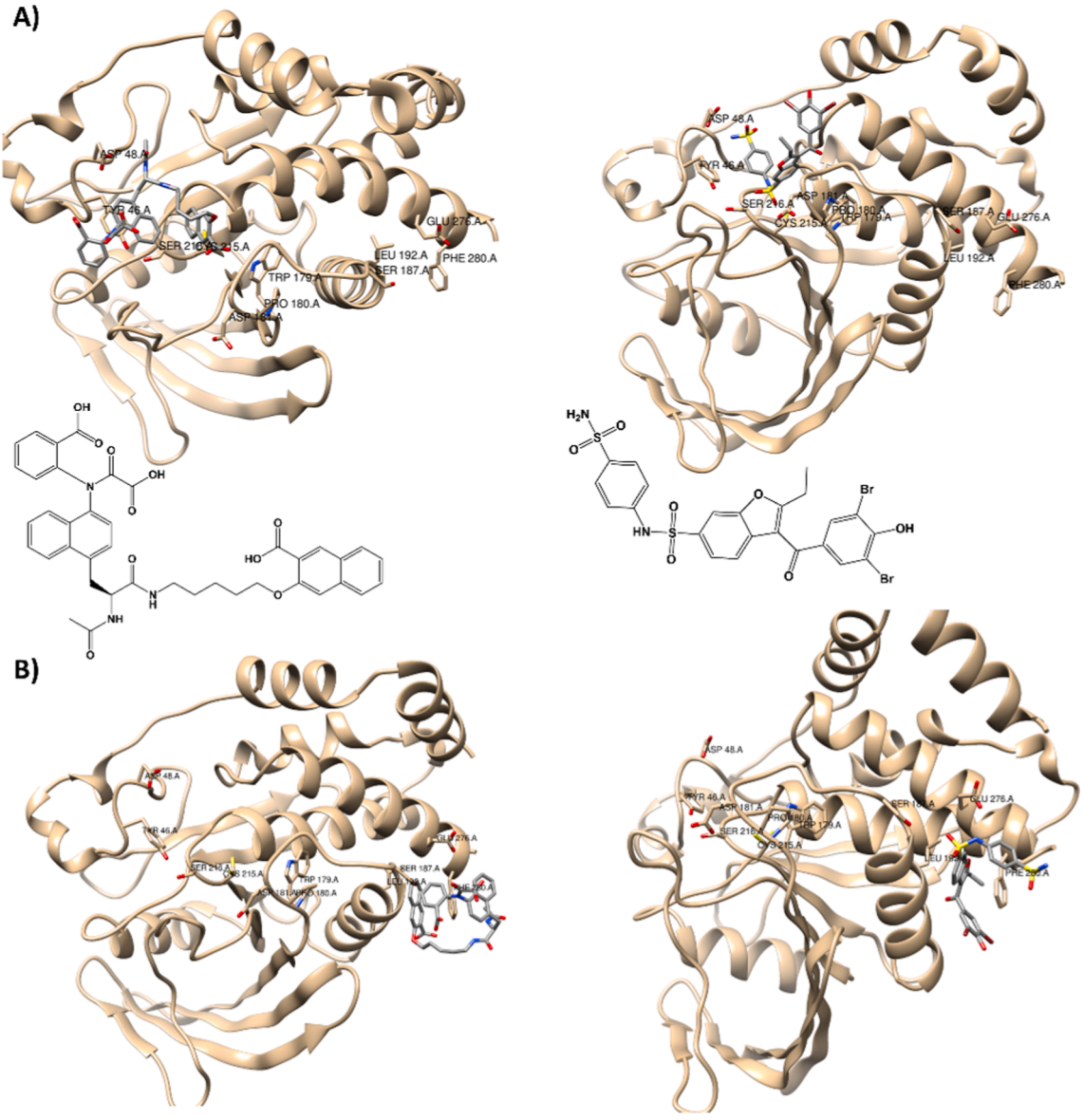

Fig. 5. Interaction profiles of the best-docked poses for the dinaphthyl and sulphonamide benzbromarone derivatives on A) catalytic site and B) allosteric site of PTP1B enzyme.

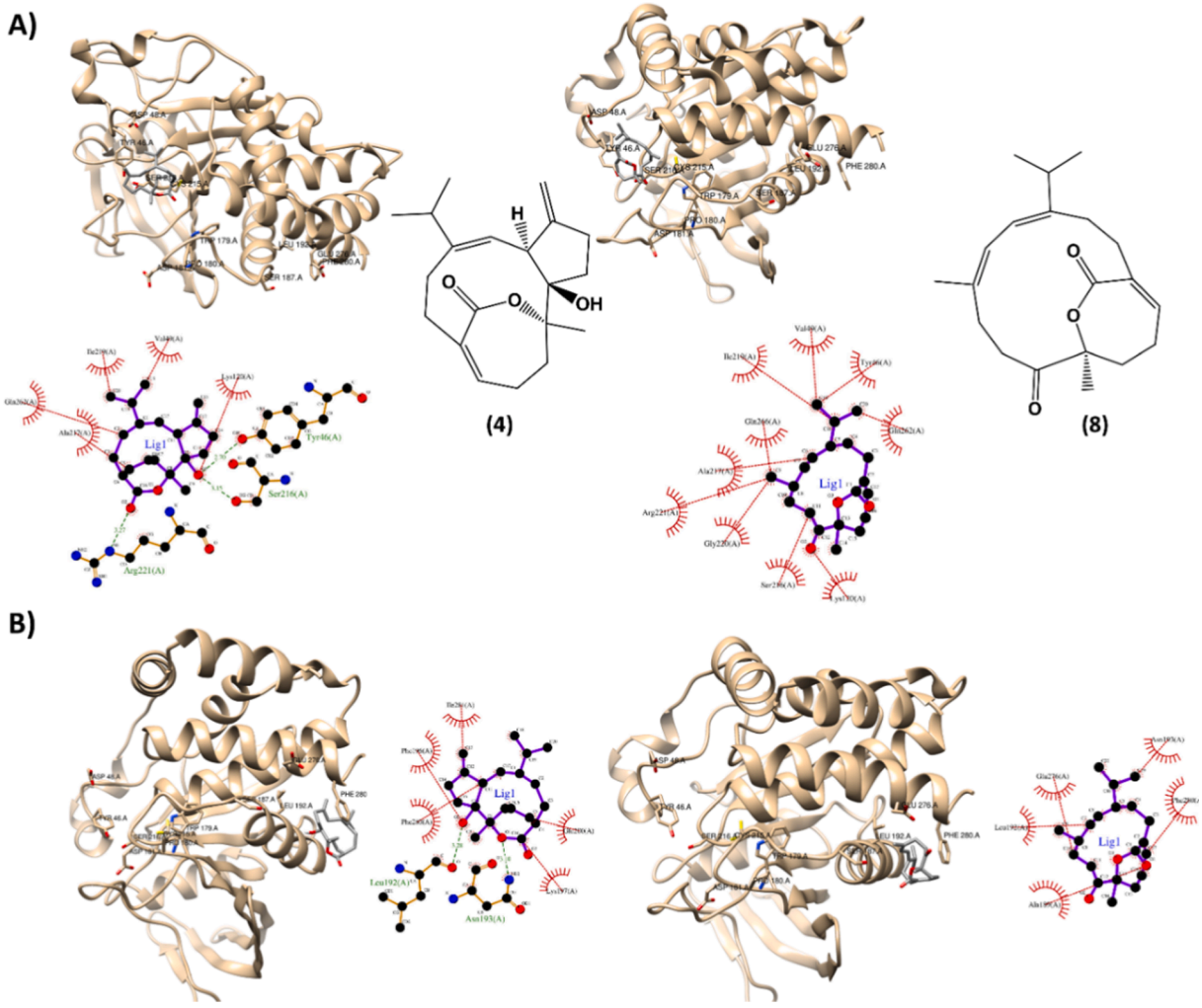

Fig. 6. Interaction profiles of the best-docked poses for the diterpene derivatives (**4**) and (**8**) on A) catalytic site and B) allosteric site of PTP1B enzyme.

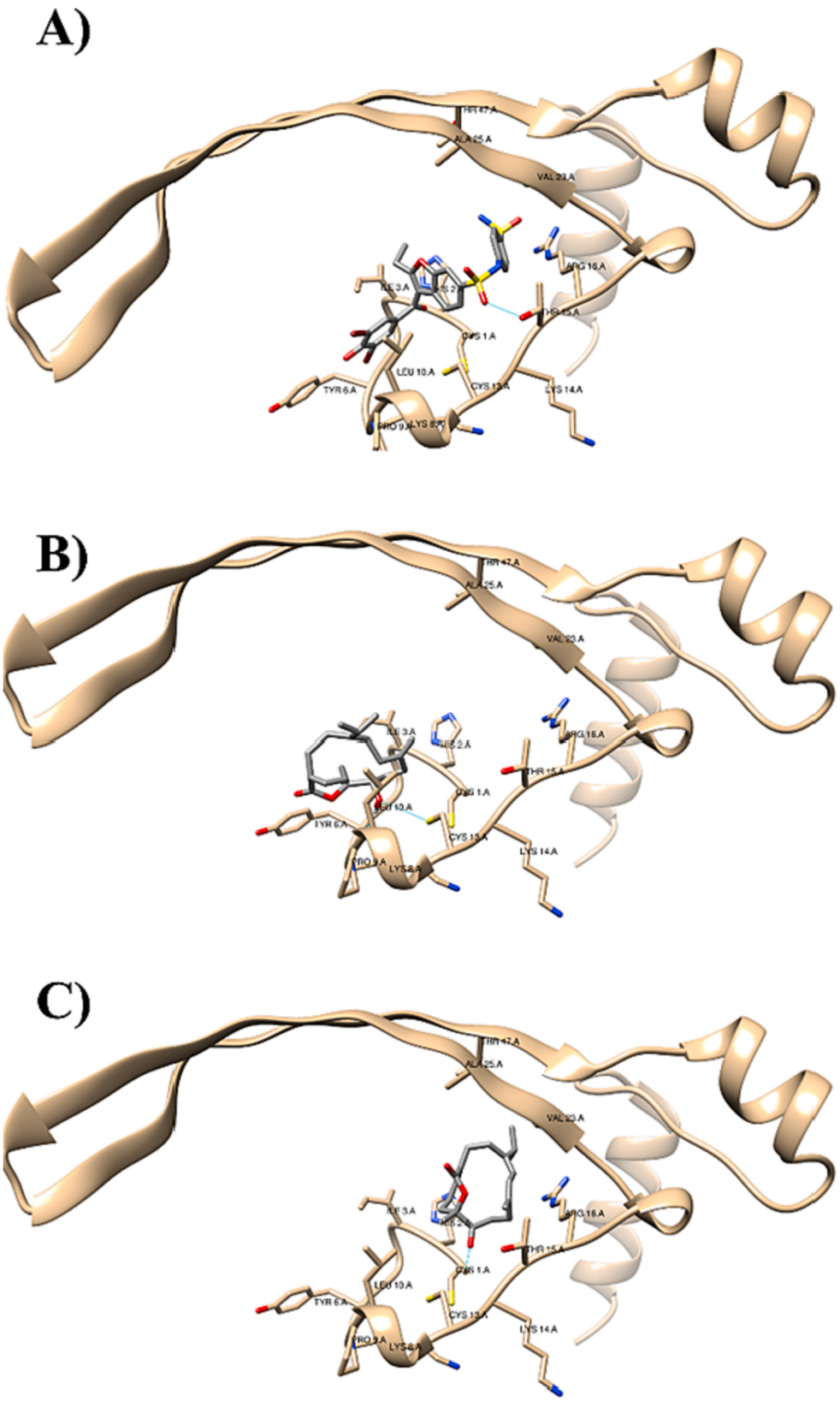

Fig. 7. Interaction profiles of the best-docked poses for the sulphonamide benzbromarone derivative (A), the diterpene derivative (**4**), (B) and the diterpene derivative (**8**), (C) of fetuin A.

Table 9
ADME/Tox profiling of six selected marine diterpenes and the two positive controls (dinaphthyl and sulphonamide benzbromarone derivatives).

ADME/Tox	4	8	9	10	13	14	Dinaphthyl	Sulphonamide benzbromarone
Lipinski #violations[1]	0	0	0	0	1	1	2	1
Veber #violations[1]	0	0	0	0	0	0	2	1
Bioavailability Score[1]	0.55	0.55	0.55	0.55	0.55	0.55	0.11	0.55
PAINS #alerts[2]	0	0	0	0	0	0	0	0
Log Po/w (XLOGP3)[3]	3.21	3.84	3.84	3.5	7.06	7.06	6.94	4.62
Log S (ESOL)[4]	−3.76	−4.16	−4.16	−4.08	−5.98	−5.98	−7.22	−6.8
GI absorption[5]	high	high	high	high	low	low	low	low
BBB permeant[5]	yes	yes	yes	yes	no	no	no	no
P-gp substrate[5]	yes	no	no	no	no	no	no	no
CYP inhibitors[5]	yes	yes	yes	yes	yes	yes	yes	yes
Log Kp (skin permeation)[5]	−5.95	−5.5	−5.5	−6.01	−2.95	−2.95	−6.4	−7.04

[1] Druglikeness. [2]Medicinal chemistry. [3]Lipophilicity. [4]Water solubility. [5]Pharmacokinetics.

selected as the most promising allosteric inhibitors of PTP1B (**4** and **8**) there is a clear interaction between these and the allosteric residues, Leu192-Phe280-Gln276, from the PTP1B enzyme as shown in Fig. 6B.

With regard to fetuin A, only the allosteric inhibitor of the PTP1B enzyme, the sulphonamide benzbromarone derivative, appears to bind more effectively to the protein, as seen by the calculated ΔG_B of −6.8 kcal/mol (Table 8). However, if we compare the best-docked poses for the most promising diterpene derivatives (**4** and **8**) with those obtained for the sulphonamide benzbromarone derivative, it can be seen that only the diterpene derivative (**8**) binds to fetuin A in a similar way, Fig. 7.

Pharmacokinetics, toxicity and druglikeness (ADME/Tox), in silico prediction

To assess the pharmacokinetics of our most promising marine diterpenes as anti-obesity agents, SwissADME (http://www.swissadme.ch/) (Daina et al., 2017), an online free tool, was used to evaluate the ADME/Tox (absorption, distribution, metabolism, excretion, and toxicity) properties of the six most promising predicted marine diterpenes (**4**, **8**, **9**, **10**, **13** and **14**). In terms of druglikeness, it was found that diterpenes (**13** and **14**) had only one Lipinski rule violation each, the other most promise diterpenes (**4**, **8**, **9**, and **10**) had no Lipinski rule violation, while the positive controls, dinaphthyl and sulphonamide benzbromarone derivatives, had two and one Lipinski rule violations, respectively (Table 9). No PAINS alert was predicted for any of the marine diterpenes or positive controls.

The Abbot bioavailability Score predicts the probability of a compound to have at least 10 % oral bioavailability in rat or measurable Caco-2 permeability, all six marine diterpenes and one of the positive controls (sulphonamide benzbromarone derivative) were predicted with a score of 55 % which is quite acceptable, while the other positive control (dinaphthyl derivative) only was predicted with a score of 11 %. All six marine diterpene derivatives and the two positive controls (dinaphthyl and sulphonamide benzbromarone derivatives) are predicted to have adequate water solubility characteristics but two of the diterpenes (**13** and **14**) and the positive control (dinaphthyl derivative) were predicted to as having high lipophilicity (>5). The targets, P-gp and CYP, seem to have a relevant role in the protection of tissues and organisms, so the interaction with them is seen positively. Thus, the diterpene (**4**) and the positive control (sulphonamide benzbromarone derivative) are predicted to be P-gp substrates and all the diterpenes (**4**, **8**, **9**, **10**, **13**, and **14**) and the positive control (dinaphthyl derivative) are predicted to inhibit at least one CYP type. The more negative the log Kp, the less skin permeant is the molecule, therefore the least skin permeant predicted is the positive control (sulphonamide benzbromarone derivative) and the most skin permeant predicted are the two diterpenes (**13** and **14**). Only for the four diterpenes (**4**, **8**, **9** and **10**) high GI absorption and blood–brain barrier penetration (related to distribution properties) were predicted.

Conclusions

Obesity is a worldwide issue that affects people of all ages, genders, and socioeconomic origins. Its prevalence has progressively increased over the last several decades. The goal of this work is to confirm the hypolipidemic impact of an organic extract of the Red Sea soft coral *Sarcophyton glaucum* in an obese rat model using biochemical and histological techniques. Our findings demonstrated a noteworthy improvement in glucose, insulin, HOMA-IR, lipid profile, fetuin B, fetuin A, PTP1B, omentin, and adropin levels, as well as UCP1 and PPARGC1A gene expression after treatment with soft coral extract and orlistat, but soft coral outperformed orlistat. These activities seem to be related to the modulation of PTP1B and fetuin A enzymes by marine diterpene derivatives that were isolated from soft coral extracts. A molecular docking study of 27 marine diterpene derivatives revealed two promising terpenoid modulators (**4** and **8**) according to their prominent ligand–protein energy scores and relevant binding affinities with the PTP1B and fetuin A pocket residues. The two selected marine diterpenes (**4** and **8**) present an α,β-unsaturated ε-caprolactone fused to a cyclic system that appears to be a key structural element to enhance anti-obesity activity. Furthermore, it can be seen by comparing the best-docked poses for the most promising diterpene derivatives (**4** and **8**) with those obtained for the sulphonamide benzbromarone derivative (positive control) that only the diterpene (**8**) binds to fetuin A in the same way as the positive control.

Institutional review board statement

The animal study protocol was approved by the Ethics Committee of National Research Center, Dokki, Cairo, Egypt, approval number (74125062023).

CRediT authorship contribution statement

Mohamed A. Tammam: Conceptualization, Methodology, Formal analysis, Investigation, Resources, Data curation, Writing – original draft, Writing – review & editing, Visualization. **Omnia Aly:** Methodology, Formal analysis, Investigation, Resources, Data curation, Writing – original draft, Writing – review & editing. **Florbela Pereira:** Methodology, Formal analysis, Investigation, Resources, Data curation, Writing – original draft, Writing – review & editing. **Aldoushy Mahdy:** Resources. **Amr El-Demerdash:** Conceptualization, Methodology, Formal analysis, Investigation, Resources, Data curation, Writing – original draft, Writing – review & editing, Visualization.

Declaration of competing interest

The authors declare that they have no known competing financial interests or personal relationships that could have appeared to influence the work reported in this paper.

Data availability

No data was used for the research described in the article.

Acknowledgments

Mohamed A. Tammam is humbly dedicating this work to the soul of his sister Dr Mai A. Tammam who passed away on 19 of March 2022, she was always a kind supporter in all aspects of his life. Florbela Pereira gratefully acknowledges FCT - Fundação para a Ciência e a Tecnologia, I. P., for an Assistant Research Position (CEECIND/01649/2021) and the project UIDB/50006/2020 of the Associated Laboratory for Green Chemistry (LAQV) of the Network of Chemistry and Technology (REQUIMTE). Amr El-Demerdash is immensely grateful to the John Innes Centre, Norwich Research Park, United Kingdom for the post-doctoral fellowship. Amr El-Demerdash is thankful to his home university, Mansoura University, Egypt for the unlimited support, inside and outside.

Appendix A. Supplementary material

Supplementary data to this article can be found online at https://doi.org/10.1016/j.crbiot.2024.100175.

References

Abdel-Wahhab, M.A., El-Nekeety, A.A., Hassan, N.S., El-Hefnawy, M.S., Kotb, M.M., El-Mekkawy, S.A., Khalil, N.A., Hanna, A.G., 2012. Hepatoprotective effect of sarcophine isolated from soft coral (Sarcophyton glaucum) in rats. Glob. Vet. 8, 244–253.

Arya, A., Nahar, L., Khan, H.U., Sarker, S.D., 2020. Anti-obesity natural products. Annu. Rep. Med. Chem. 55, 411–433. https://doi.org/10.1016/BS.ARMC.2020.02.006.

Badawy, E., El-laithy, N.A., Morsy, S.M., Ashour, M.N., Elias, T.R., Masoud, M.M., Aly, O., 2020. Role of swimming on muscle PGC-1α, FNDC5 mRNA, and assessment of serum omentin, adropin, and irisin in high carbohydrate high fat (HCHF) diet induced obesity in rats. Egypt J. Med. Hum. Genet. 21, 1–8. https://doi.org/10.1186/S43042-020-00080-6/FIGURES/2.

Becke, A.D., 1993a. A new mixing of hartree-fock and local density-functional theories. J. Chem. Phys. 98, 1372–1377. https://doi.org/10.1063/1.464304.

Becke, A.D., 1993b. Density-functional thermochemistry. III. The role of exact exchange. J. Chem. Phys. 98, 5648–5652. https://doi.org/10.1063/1.464913.

Bettini, S., Favaretto, F., Compagnin, C., Belligoli, A., Sanna, M., Fabris, R., Serra, R., Dal Prà, C., Prevedello, L., Foletto, M., Vettor, R., Milan, G., Busetto, L., 2019. Resting energy expenditure, insulin resistance and UCP1 expression in human subcutaneous and visceral adipose tissue of patients with obesity. Front. Endocrinol. (Lausanne) 10, 548. https://doi.org/10.3389/FENDO.2019.00548.

Bourebaba, L., Kornicka-Garbowska, K., Al Naem, M., Röcken, M., Łyczko, J., Marycz, K., 2021. MSI-1436 improves EMS adipose derived progenitor stem cells in the course of adipogenic differentiation through modulation of ER stress, apoptosis, and oxidative stress. Stem Cell Res. Ther. 12, 1–18. https://doi.org/10.1186/S13287-020-02102-X/TABLES/2.

Bourebaba, L., Marycz, K., 2019. Pathophysiological implication of fetuin-A glycoprotein in the development of metabolic disorders: A concise review. J. Clin. Med. 8, 2033. https://doi.org/10.3390/JCM8122033.

Chait, A., den Hartigh, L.J., 2020. Adipose tissue distribution, inflammation and its metabolic consequences, including diabetes and cardiovascular disease. Front. Cardiovasc. Med. 7, 22. https://doi.org/10.3389/FCVM.2020.00022.

Cole, T.G., Kuisk, I., Patsch, W., Schonfeld, G., 1984. Effects of high cholesterol diets on rat plasma lipoproteins and lipoprotein-cell interactions. J. Lipid Res. 25, 593–603. https://doi.org/10.1016/S0022-2275(20)37772-5.

Cuppari, A., Körschgen, H., Fahrenkamp, D., Schmitz, C., Guevara, T., Karmilin, K., Kuske, M., Olf, M., Dietzel, E., Yiallouros, I., De Sanctis, D., Goulas, T., Weiskirchen, R., Jahnen-Dechent, W., Floehr, J., Stoecker, W., Jovine, L., Xavier Gomis-Rüth, F., 2019. Structure of mammalian plasma fetuin-B and its mechanism of selective metallopeptidase inhibition. IUCrJ 6, 317–330. https://doi.org/10.1107/S2052252519001568.

Daina, A., Michielin, O., Zoete, V., 2017. SwissADME: a free web tool to evaluate pharmacokinetics, drug-likeness and medicinal chemistry friendliness of small molecules. Sci. Rep. 7, 1–13. https://doi.org/10.1038/srep42717.

De Souza Batista, C.M., Yang, R.Z., Lee, M.J., Glynn, N.M., Yu, D.Z., Pray, J., Ndubuizu, K., Patil, S., Schwartz, A., Kligman, M., Fried, S.K., Gong, D.W., Shuldiner, A.R., Pollin, T.I., McLenithan, J.C., 2007. Omentin plasma levels and gene expression are decreased in obesity. Diabetes 56, 1655–1661. https://doi.org/10.2337/DB06-1506.

Friedewald, W.T., Levy, R.I., Fredrickson, D.S., 1972. Estimation of the concentration of low-density lipoprotein cholesterol in plasma, without use of the preparative ultracentrifuge. Clin. Chem. 18, 499–502.

Frisch, M.J., Robb, M.A., Cheeseman, J.R., Scalmani, G., Barone, V., Mennucci, B., Petersson, G.A., Nakatsuji, H., Caricato, M., Li, X., et al., 2010. Gaussian 09, Revision B.01. Gaussian Inc., Wallingford.

Ganesh Kumar, K., Zhang, J., Gao, S., Rossi, J., McGuinness, O.P., Halem, H.H., Culler, M.D., Mynatt, R.L., Butler, A.A., 2012. Adropin deficiency is associated with increased adiposity and insulin resistance. Obesity 20, 1394–1402. https://doi.org/10.1038/OBY.2012.31.

Ghareeb, M.A., Tammam, M.A., El-Demerdash, A., Atanasov, A.G., 2020. Insights about clinically approved and Preclinically investigated marine natural products. Curr. Res. Biotechnol. 2, 88–102. https://doi.org/10.1016/J.CRBIOT.2020.09.001.

Gustafsson, D., Unwin, R., 2013. The pathophysiology of hyperuricaemia and its possible relationship to cardiovascular disease, morbidity and mortality. BMC Nephrol. 14, 1–9. https://doi.org/10.1186/1471-2369-14-164/FIGURES/1.

Hayashi, M., Morioka, T., Hatamori, M., Kakutani, Y., Yamazaki, Y., Kurajoh, M., Motoyama, K., Mori, K., Fukumoto, S., Shioi, A., Shoji, T., Emoto, M., Inaba, M., 2019. Plasma omentin levels are associated with vascular endothelial function in patients with type 2 diabetes at elevated cardiovascular risk. Diabetes Res. Clin. Pract. 148, 160–168. https://doi.org/10.1016/j.diabres.2019.01.009.

Health, T.L.P., 2023. Obesity prevention: changing perspectives. Lancet Public Health 8, e161.

Huang, M., Claussnitzer, M., Saadat, A., Coral, D.E., Kalamajski, S., Franks, P.W., 2023. Engineered allele substitution at PPARGC1A rs8192678 alters human white adipocyte differentiation, lipogenesis, and PGC-1α content and turnover. Diabetologia 66, 1289. https://doi.org/10.1007/S00125-023-05915-6.

Huang, T.Y., Huang, C.Y., Chen, S.R., Weng, J.R., Tu, T.H., Cheng, Y.B., Wu, S.H., Sheu, J.H., 2020. New hydroquinone monoterpenoid and cembranoid-related metabolites from the soft coral *Sarcophyton tenuispiculatum*. Mar. Drugs 19, 8. https://doi.org/10.3390/MD19010008.

Jumper, J., Evans, R., Pritzel, A., Green, T., Figurnov, M., Ronneberger, O., Tunyasuvunakool, K., Bates, R., Žídek, A., Potapenko, A., Bridgland, A., Meyer, C., Kohl, S.A.A., Ballard, A.J., Cowie, A., Romera-Paredes, B., Nikolov, S., Jain, R., Adler, J., Back, T., Petersen, S., Reiman, D., Clancy, E., Zielinski, M., Steinegger, M., Pacholska, M., Berghammer, T., Bodenstein, S., Silver, D., Vinyals, O., Senior, A.W., Kavukcuoglu, K., Kohli, P., Hassabis, D., 2021. Highly accurate protein structure prediction with AlphaFold. Nature 596, 583–589. https://doi.org/10.1038/s41586-021-03819-2.

Jung, U.J., Choi, M.S., 2014. Obesity and Its Metabolic Complications: The Role of adipokines and the relationship between obesity, inflammation, insulin resistance, dyslipidemia and nonalcoholic fatty liver disease. Int. J. Mol. Sci. 15, 6184–6223. https://doi.org/10.3390/IJMS15046184.

Kelstrup, L., Hjort, L., Houshmand-Oeregaard, A., Clausen, T.D., Hansen, N.S., Broholm, C., Borch-Johnsen, L., Mathiesen, E.R., Vaag, A.A., Damm, P., 2016. Gene expression and DNA methylation of PPARGC1A in muscle and adipose tissue from adult offspring of women with diabetes in pregnancy. Diabetes 65, 2900–2910. https://doi.org/10.2337/DB16-0227.

Kim, K.-O., Kim, Y.-A., Lee, H., 2007. Isoflavone-rich bean sprout cookie improves lipid metabolism in hyperlipidemic rat. FASEB J. 21, A1087–A. https://doi.org/10.1096/FASEBJ.21.6.A1087-A.

Kumar, K.G., Trevaskis, J.L., Lam, D.D., Sutton, G.M., Koza, R.A., Chouljenko, V.N., Kousoulas, K.G., Rogers, P.M., Kesterson, R.A., Thearle, M., Ferrante, A.W., Mynatt, R.L., Burris, T.P., Dong, J.Z., Halem, H.A., Culler, M.D., Heisler, L.K., Stephens, J.M., Butler, A.A., 2008. identification of adropin as a secreted factor linking dietary macronutrient intake with energy homeostasis and lipid metabolism. Cell Metab. 8, 468. https://doi.org/10.1016/J.CMET.2008.10.011.

Levesque, R., 2005. SPSS programming and data management: A guide for SPSS and SAS users. Ibm Spss 1–520.

Li, M., Chi, X., Wang, Y., Setrerrahmane, S., Xie, W., Xu, H., 2022. Trends in insulin resistance: insights into mechanisms and therapeutic strategy. Signal. Transduct. Target Ther. 7, 216. https://doi.org/10.1038/S41392-022-01073-0.

Liang, L.F., Gao, L.X., Li, J., Taglialatela-Scafati, O., Guo, Y.W., 2013a. Cembrane diterpenoids from the soft coral *Sarcophyton trocheliophorum* Marenzeller as a new class of PTP1B inhibitors. Bioorg. Med. Chem. 21, 5076–5080. https://doi.org/10.1016/J.BMC.2013.06.043.

Liang, L.F., Guo, Y.W., 2013. Terpenes from the soft corals of the Genus *Sarcophyton*: Chemistry and biological activities. Chem. Biodivers. 10, 2161–2196. https://doi.org/10.1002/CBDV.201200122.

Liang, L.F., Kurtán, T., Mándi, A., Yao, L.G., Li, J., Zhang, W., Guo, Y.W., 2013b. Unprecedented diterpenoids as a PTP1B inhibitor from the Hainan soft coral *Sarcophyton trocheliophorum* Marenzeller. Org. Lett. 15, 274–277. https://doi.org/10.1021/OL303110D.

Liang, L.F., Kurtán, T., Mándi, A., Gao, L.X., Li, J., Zhang, W., Guo, Y.W., 2014. Sarsolenane and capnosane diterpenes from the Hainan soft coral *Sarcophyton trocheliophorum* Marenzeller as PTP1B Inhibitors. Eur. J. Org. Chem. 2014, 1841–1847. https://doi.org/10.1002/EJOC.201301683.

Liu, R., Mathieu, C., Berthelet, J., Zhang, W., Dupret, J.M., Rodrigues Lima, F., 2022. Human protein tyrosine phosphatase 1B (PTP1B): From structure to clinical inhibitor perspectives. Int. J. Mol. Sci. 23, 7027. https://doi.org/10.3390/IJMS23137027.

Livak, K.J., Schmittgen, T.D., 2001. analysis of relative gene expression data using real-time quantitative PCR and the 2−ΔΔCT Method. Methods 25, 402–408. https://doi.org/10.1006/METH.2001.1262.

Lopes Virella, M.F., Stone, P., Ellis, S., Colwell, J.A., 1977. Cholesterol determination in high-density lipoproteins separated by three different methods. Clin. Chem. 23, 882–884. https://doi.org/10.1093/CLINCHEM/23.5.882.

Maliszewska, K., Kretowski, A., 2021. brown adipose tissue and its role in insulin and glucose homeostasis. Int. J. Mol. Sci. 22, 1530. https://doi.org/10.3390/IJMS22041530.

MarinLit - A database of the marine natural products literature. https://marinlit.rsc.org/ (accessed 9.30.23).
Matthews, D.R., Hosker, J.P., Rudenski, A.S., Naylor, B.A., Treacher, D.F., Turner, R.C., 1985. Homeostasis model assessment: insulin resistance and beta-cell function from fasting plasma glucose and insulin concentrations in man. Diabetologia 28, 412–419. https://doi.org/10.1007/BF00280883.
Mohammad, N.S., Nazli, R., Zafar, H., Fatima, S., 2022. Effects of lipid based Multiple Micronutrients Supplement on the birth outcome of underweight pre-eclamptic women: A randomized clinical trial. Pak. J. Med. Sci. 38, 219–226. https://doi.org/10.12669/PJMS.38.1.4396.
Ngoc, N.T., Hanh, T.T.H., Quang, T.H., Cuong, N.X., Nam, N.H., Thao, D.T., Thung, D.C., Kiem, P.V., Minh, C.V., 2021. Polyhydroxylated steroids from the Vietnamese soft *coral Sarcophyton ehrenbergi*. Steroids 176, 108932. https://doi.org/10.1016/J.STEROIDS.2021.108932.
O'Boyle, N.M., Banck, M., James, C.A., Morley, C., Vandermeersch, T., Hutchison, G.R., 2011. Open Babel: An open chemical toolbox. J. Cheminform. 3 https://doi.org/10.1186/1758-2946-3-33.
Paget, G., Thomson, R., 1979. Standard operating procedures in pathology: including developmental toxicology and quality assurance.
Passing, H., Bablok, W., 1983. A new biometrical procedure for testing the equality of measurements from two different analytical methods. Application of linear regression procedures for method comparison studies in clinical chemistry, Part I. J. Clin. Chem. Clin. Biochem. 21, 709–720. https://doi.org/10.1515/CCLM.1983.21.11.709.
Pettersen, E.F., Goddard, T.D., Huang, C.C., Couch, G.S., Greenblatt, D.M., Meng, E.C., Ferrin, T.E., 2004. UCSF Chimera–a visualization system for exploratory research and analysis. J. Comput. Chem. 25, 1605–1612. https://doi.org/10.1002/JCC.20084.
Poloczek, J., Tarnawska, M., Chełmecka, E., Łaszczyca, P., Gumprecht, J., Stygar, D., 2021. High fat, high sugar diet and djos bariatric surgery influence plasma levels of fetuin-b, growth differentiation factor-15, and pentraxin 3 in diet-induced obese sprague–dawley rats. Nutrients 13, 3632. https://doi.org/10.3390/NU13103632.
Ramírez-Vélez, R., García-Hermoso, A., Hackney, A.C., Izquierdo, M., 2019. Effects of exercise training on Fetuin-a in obese, type 2 diabetes and cardiovascular disease in adults and elderly: a systematic review and Meta-analysis. Lipids Health Dis. 18, 23. https://doi.org/10.1186/S12944-019-0962-2.
Reeves, P.G., 1997. Components of the AIN-93 diets as improvements in the AIN-76A diet. J. Nutr. 127, 838S–841S. https://doi.org/10.1093/JN/127.5.838S.
Rudloff, S., Janot, M., Rodriguez, S., Dessalle, K., Jahnen-Dechent, W., Huynh-Do, U., 2021. Fetuin-A is a HIF target that safeguards tissue integrity during hypoxic stress. Nat. Commun. 12, 1–16. https://doi.org/10.1038/s41467-020-20832-7.
Rudloff, S., Jahnen-Dechent, W., Huynh-Do, U., 2022. Tissue chaperoning-the expanded functions of fetuin-A beyond inhibition of systemic calcification. Pflugers Arch. 474, 949–962. https://doi.org/10.1007/S00424-022-02688-6.
Schirinzi, V., Poli, C., Berteotti, C., Leone, A., 2023. Browning of adipocytes: a potential therapeutic approach to obesity. Nutrients 15, 2229. https://doi.org/10.3390/NU15092229.
Sharma, B., Xie, L., Yang, F., Wang, W., Zhou, Q., Xiang, M., Zhou, S., Lv, W., Jia, Y., Pokhrel, L., Shen, J., Xiao, Q., Gao, L., Deng, W., 2020. Recent advance on PTP1B inhibitors and their biomedical applications. Eur. J. Med. Chem. 199, 112376 https://doi.org/10.1016/J.EJMECH.2020.112376.
Sohail, A., Fayyaz, H., Muneer, H., Raza, I., Ikram, M., Uddin, Z., Gul, S., Almohaimeed, H.M., Alsharif, I., Alaryani, F.S., Ullah, I., 2022. targeted inhibition of protein tyrosine phosphatase 1b by viscosol ameliorates type 2 diabetes pathophysiology and histology in diabetic mouse model. Biomed. Res. Int. 2022 https://doi.org/10.1155/2022/2323078.
Song, Y.T., Yu, D.D., Su, M.Z., Luo, H., Cao, J.G., Liang, L.F., Yang, F., Guo, Y.W., 2023. Structurally diverse diterpenes from the South China Sea soft coral *Sarcophyton trocheliophorum*. Mar. Drugs 21, 69. https://doi.org/10.3390/MD21020069/S1.
Soppert, J., Lehrke, M., Marx, N., Jankowski, J., Noels, H., 2020. Lipoproteins and lipids in cardiovascular disease: from mechanistic insights to therapeutic targeting. Adv. Drug Deliv. Rev. 159, 4–33. https://doi.org/10.1016/J.ADDR.2020.07.019.
Stygar, D., Sawczyn, T., Skrzep-Poloczek, B., Owczarek, A.J., Matysiak, N., Michalski, M., Mielańczyk, Ł., Bażanów, B., Ziora, P., Choręza, P., Doleżych, B., Karcz, K.W., 2018. The effects of duodenojejunal omega switch in combination with high-fat diet and control diet on incretins, body weight, and glucose tolerance in sprague-dawley rats. Obes. Surg. 28, 748–759. https://doi.org/10.1007/S11695-017-2883-3/FIGURES/5.
SwissADME. http://www.swissadme.ch/ (accessed 9.7.23).
Szczepankiewicz, B.G., Liu, G., Hajduk, P.J., Abad-Zapatero, C., Pei, Z., Xin, Z., Lubben, T.H., Trevillyan, J.M., Stashko, M.A., Ballaron, S.J., Liang, H., Huang, F., Hutchins, C.W., Fesik, S.W., Jirousek, M.R., 2003. Discovery of a potent, selective protein tyrosine phosphatase 1B inhibitor using a linked-fragment strategy. J. Am. Chem. Soc. 125, 4087–4096. https://doi.org/10.1021/JA0296733.
Tammam, M.A., El-Demerdash, A., 2023. Pederins, mycalamides, onnamides and theopederins: Distinctive polyketide families with intriguing therapeutic potentialities. Curr. Res. Biotechnol. 6, 100145 https://doi.org/10.1016/J.CRBIOT.2023.100145.
Tammam, M.A., Pereira, F., Aly, O., Sebak, M., Diab, Y.M., Mahdy, A., El-Demerdash, A., 2023. Investigating the hepatoprotective potentiality of marine-derived steroids as promising inhibitors of liver fibrosis. RSC Adv 13, 27477–27490. https://doi.org/10.1039/D3RA04843H.
Tan, B.K., Pua, S., Syed, F., Lewandowski, K.C., O'Hare, J.P., Randeva, H.S., 2008. Decreased plasma omentin-1 levels in Type 1 diabetes mellitus. Diabetic Med. 25, 1254–1255. https://doi.org/10.1111/J.1464-5491.2008.02568.X.
Topuz, M., Celik, A., Aslantas, T., Demir, A.K., Aydin, S., Aydin, S., 2013. Plasma adropin levels predict endothelial dysfunction like flow-mediated dilatation in patients with type 2 diabetes mellitus. J. Investig. Med. 61, 1161–1164. https://doi.org/10.2310/JIM.0000000000000003.
Trott, O., Olson, A.J., 2010. AutoDock Vina: improving the speed and accuracy of docking with a new scoring function, efficient optimization, and multithreading. J. Comput. Chem. 31, NA-NA. https://doi.org/10.1002/JCC.21334.
Varadi, M., Anyango, S., Deshpande, M., Nair, S., Natassia, C., Yordanova, G., Yuan, D., Stroe, O., Wood, G., Laydon, A., Zídek, A., Green, T., Tunyasuvunakool, K., Petersen, S., Jumper, J., Clancy, E., Green, R., Vora, A., Lutfi, M., Figurnov, M., Cowie, A., Hobbs, N., Kohli, P., Kleywegt, G., Birney, E., Hassabis, D., Velankar, S., 2022. AlphaFold protein structure database: massively expanding the structural coverage of protein-sequence space with high-accuracy models. Nucleic Acids Res. 50, D439–D444. https://doi.org/10.1093/NAR/GKAB1061.
Wallace, A.C., Laskowski, R.A., Thornton, J.M., 1995. LIGPLOT: a program to generate schematic diagrams of protein-ligand interactions. Protein Eng. 8, 127–134. https://doi.org/10.1093/PROTEIN/8.2.127.
Wang, S.K., Hsieh, M.K., Duh, C.Y., 2012. Three new cembranoids from the Taiwanese soft coral *Sarcophyton ehrenbergi*. Mar. Drugs 10, 1433–1444. https://doi.org/10.3390/MD10071433.
Wang, D., Wu, M., Zhang, X., Li, L., Lin, M., Shi, X., Zhao, Y., Huang, C., Li, X., 2022. Hepatokine fetuin B expression is regulated by leptin-STAT3 signalling and associated with leptin in obesity. Sci. Rep. 12, 12869. https://doi.org/10.1038/S41598-022-17000-W.
Weber, C., Noels, H., 2011. Atherosclerosis: current pathogenesis and therapeutic options. Nat. Med. 17, 1410–1422. https://doi.org/10.1038/NM.2538.
Wiesmann, C., Barr, K.J., Kung, J., Zhu, J., Erlanson, D.A., Shen, W., Fahr, B.J., Zhong, M., Taylor, L., Randall, M., McDowell, R.S., Hansen, S.K., 2004. Allosteric inhibition of protein tyrosine phosphatase 1B. Nat. Struct. Mol. Biol. 11, 730–737. https://doi.org/10.1038/NSMB803.
Wilfinger, W.W., Mackey, K., Chomczynski, P., 1997. Effect of pH and ionic strength on the spectrophotometric assessment of nucleic acid purity. Biotechniques 22, 474–481. https://doi.org/10.2144/97223ST01.
Wilson, C.R., Tran, M.K., Salazar, K.L., Young, M.E., Taegtmeyer, H., 2007. Western diet, but not high fat diet, causes derangements of fatty acid metabolism and contractile dysfunction in the heart of Wistar rats. Biochem. J. 406, 457–467. https://doi.org/10.1042/BJ20070392.
Yalow, R., Bauman W. A, 1983. Insulin in health and disease, In: Diabetes Mellitus: Theory and Practice. Excerpta Medica, New York.
Yang, Y., Zhang, L., Tian, J., Ye, F., Xiao, Z., 2021. Integrated approach to identify selective PTP1B inhibitors targeting the allosteric site. J. Chem. Inf. Model. 61, 4720–4732. https://doi.org/10.1021/ACS.JCIM.1C00357.
Zaitone, S.A., Essawy, S., 2012. Addition of a low dose of rimonabant to orlistat therapy decreases weight gain and reduces adiposity in dietary obese rats. Clin. Exp. Pharmacol. Physiol. 39, 551–559. https://doi.org/10.1111/J.1440-1681.2012.05717.X.
Zengi, S., Zengi, O., Kirankaya, A., Kucuk, S.H., Kutanis, E.E., Yigit, O., 2019. Serum omentin-1 levels in obese children. J. Pediatr. Endocrinol. Metab. 32, 247–251. https://doi.org/10.1515/JPEM-2018-0231.
Zhang, H., Chen, N., 2022. Adropin as an indicator of T2DM and its complications. Food Sci. Hum. Well 11, 1455–1463. https://doi.org/10.1016/J.FSHW.2022.06.002.